Hamidreza Shariatmadari

Channel ranking scheme in wireless sensor networks based on packet delivery ratio estimation

School of Electrical Engineering

Thesis submitted for examination for the degree of Master of Science in Technology.

Espoo 1.4.2012

Thesis supervisor:

Prof. Riku Jäntti

Thesis instructor:

M.Sc. Aamir Mahmood

Aalto University
School of Electrical
Engineering

AALTO UNIVERSITY
SCHOOL OF ELECTRICAL ENGINEERING

ABSTRACT OF THE
MASTER'S THESIS

Author: Hamidreza Shariatmadari

Title: Channel ranking scheme in wireless sensor networks based on packet delivery ratio estimation

Date: 1.4.2012 Language: English Number of pages:12+71

Department of Communications and Networking

Professorship: Radio Communications Code: S-72

Supervisor: Prof. Riku Jäntti

Instructor: M.Sc. Aamir Mahmood

The widespread deployment of competitive wireless technologies in the 2.4 GHz unlicensed Industrial, Scientific, Medical (ISM) band has introduced co-existence issues between different wireless devices. Co-channel interference severely affects the performance of Wireless Sensor Networks (WSNs) that are limited to low transmission power and low data rate. This problem can be mitigated by searching the candidate channels and choosing ones for operation which provide more reliable connection.

In this thesis, a Packet Delivery Ratio (PDR) estimation algorithm is proposed that can be used by WSNs operating in license free bands in order to rank the channels. Since the PDR is a function of Signal to Interference plus Noise Ratio at receiver node and the traffic pattern of the interferer, receiver node predicts the achievable PDR on each channel according to received signal strength from transmitter node, noise and interference characteristics obtained through spectrum measurements. Finally, channels are ranked based on achieved estimates.

The PDR estimation algorithm is implemented on the IEEE 802.15.4-based wireless sensor platform in order to assess its performance. Wireless channels are emulated to model different environments and the accuracy of PDR estimates are observed under different channel conditions. It is beneficial to minimize the energy consumption of channel scanning by reducing the number of collected samples from the channel, while the desired accuracy is fulfilled for channel ranking purpose. Hence effect of number of collected samples on performance of estimates is investigated. The channel ranking method is also evaluated in a real environment to rank IEEE 802.15.4 candidate channels in existence of interference from multiple wireless devices in 2.4 GHz frequency band.

Keywords: IEEE 802.15.4, IEEE 802.11, WSN, WLAN, Channel Ranking, Co-existence, Interference avoidance, ISM-Band

Acknowledgments

First and foremost, I would like to express my deepest thanks and gratitude to my supervisor Professor Riku Jäntti who has supported me throughout my thesis with his patience, motivation and immense knowledge whilst allowing me the room to work in my own way.

I am heartily thankful to my instructor Aamir Mahmood whose encouragement, supervision and support from the preliminary to the concluding level enabled me to develop an understanding of the subject.

I am also very grateful to Viktor Nässi for his suggestions and insightful discussions to support me in mastering various testing equipments and implementing the test-bed setup.

I would like to thank my family, who encouraged me to continue my education; without them this thesis would not have been possible to finish.

Hamidreza Shariatmadari

Otaniemi, 1.4.2012

Contents

Abbreviations and Acronyms

ABB	Analog Baseband
ACK	Acknowledgment
ADC	Analog to Digital Converter
AILS	Automatic Input Level Setting
AP	Access Point
API	Application Programming Interface
ASK	Amplitude Shift Keying
AWGN	Additive White Gaussian Noise
BER	Bit Error Rate
BPSK	Binary Phase Shift Keying
CA	Collision Avoidance
CAP	Contention Access Period
CCA	Clear Channel Assessment
CCK	Complementary Code Keying
CD	Collision Detection
CFP	Contention Free Period
CPLD	Complex Programmable Logic Device
CPU	Central Processing Unit
CSMA	Carrier Sense Multiple Access
CTS	Clear to Send
DAC	Digital to Analog Converter
DBB	Digital Baseband
DCF	Distributed Coordination Function
DSA	Dynamic Spectrum Access
DSP	Digital Signal Processing
DIFS	DCF Interframe Space
DSSS	Direct Sequence Spread Spectrum
ED	Energy Detection
FHSS	Frequency Hopping Spread Spectrum
FFD	Full-Function Device
GTS	Guaranteed Time Slot
GUI	Graphical User Interface
ICMP	Internet Control Message Protocol
IFS	Interframe Space
IoT	Internet of Things
IP	Internet Protocol
IR	Infrared
ISM	Industrial, Scientific and Medical
LAN	Local Area Network
LOS	Line-of-Sight
LR-WPAN	Low-Rate Wireless Personal Area Network
LQI	Link Quality Indicator
MAC	Media Access Control

MAN	Metropolitan Area Network
MCU	Micro Controller Unit
MFR	MAC Footer
MGEN	Multi-Generator
MHR	MAC Header
MIMO	Multiple-Input Multiple-Output
MLME	MAC Sublayer Management Entity
MMCX	Micro-Miniature Coaxial
MPDU	MAC Protocol Data Unit
MSK	Minimum Shift Keying
NAV	Network Allocation Vector
NLOS	Non-Line-of-Sight
OFDM	Orthogonal Frequency Division Multiplexing
O-QPSK	Offset-Quadrature Phase Shift Keying
PAN	Personal Area Network
PBCC	Packet Binary Convolutional Coding
PC	Point Coordinator
PCF	Point Coordination Function
PCI	Peripheral Component Interconnect
PCM	Power Control Management
PDR	Packet Delivery Ratio
PDU	Protocol Data Unit
PER	Packet Error Rate
PHY	Physical
PHR	PHY Header
PIFS	PCF Interframe Space
PN	Pseudo Noise
POSIX	Portable Operating System Interface
PPDU	PHY Protocol Data Unit
PSDU	Physical Service Data Unit
PSSS	Parallel Sequence Spread Spectrum
QAM	Quadrature Amplitude Modulation
QoS	Quality of Service
QPSK	Quadrature Phase Shift Keying
RFD	Reduced-Function Device
RISC	Reduced Instruction Set Computer
RSSI	Received Signal Strength Indicator
RTS	Request to Send
RX	Receive
SAP	Service Access Point
SHR	Synchronization Header
SIFS	Short Interframe Space
SIR	Signal to Interference Ratio
SINR	Signal to Interference plus Noise Ratio
SISO	Single-Input Single-Output

SMA	Sub Miniature version A
SNR	Signal to Noise Ratio
SSI	Simple Sensor Interface
TAG	Technical Advisory Group
TCP	Transmission Control Protocol
TDL	Tapped Delay Line
TG	Task Group
TGn	Task Group next Generation
TX	Transmit
UDP	User Datagram Protocol
UART	Universal Asynchronous Receiver/Transmitter
VoIP	Voice over IP
WLAN	Wireless Local Area Network
WPAN	Wireless Personal Area Network
WSN	Wireless Sensor Network

List of Figures

List of Tables

1 Introduction

This section presents the motivation of this thesis, reviews the related research works and states the channel ranking problems. In addition, the objectives and methodology are expressed. Finally, the thesis structure is provided.

1.1 Motivation

Interest in wireless technologies has experienced explosive growth in recent years. WSN operating in unlicensed ISM bands with special features like low power consumption has found its way into a wide variety of applications and systems [1]. WSNs are used in vastly different areas like industrial monitoring and control, building automation, traffic control, forest fire detection, machine health monitoring and so many others. Among different ISM frequency bands, the 2.4 GHz is globally accepted and widely used by WSNs. The 2.4 GHz band is divided into 16 non-overlapping channels which nodes can choose for their communication.

Unlicensed nature of 2.4 GHz band made this spectrum popular for other technologies to operate on it. Wireless Personal Area Network (WPAN), bluetooth, cordless phone are some of the other technologies that utilize this frequency band for their operation. Wireless sensor networks can easily be corrupted by transmissions of collocated wireless devices due to low transmission power of sensor nodes [2]. Therefore, WSNs should overcome numerous issues and challenges to provide requirements for underlying applications. These challenges have been further exacerbated by two new industrial wireless standards, WirelessHART [3] and ISA-SP100 [4], which need to have special industry requirements.

Since interference is inevitable in ISM bands, providing some intelligence for sensor nodes to scan candidate channels and find proper channels for operation, in term of their suitability for sensor link, can significantly improve the performance and reliability of network. This procedure helps to utilize resources in a better way and achieve the better coexistence between different wireless technologies. This thesis presents a new PDR estimation method that can be employed by WSN nodes in order to rank the channels.

1.2 Previous Work

Much research effort already has been devoted to the coexistence of wireless networks in unlicensed ISM frequency bands, especially in the 2.4 GHz band. In [5], an empirical study shows that the effects of IEEE 802.11 with high duty cycle on IEEE 802.15.4 can be severe and leads to high packet drop in the system. It is also concluded that a scheme to change channel is vital to mitigate the interference from other wireless devices. In [6], it is observed that Received Signal Strength Indicator (RSSI) provided by an IEEE 802.15.4 compliant radio transceiver chip can be used as a promising indicator of link quality if its value is above the sensitivity threshold.

It also noticed that Link Quality Indicator (LQI) should be averaged over many packets to be a reliable indicator for link quality.

In [7, 8, 9] different methods have been suggested to find the least interfered channel. In [7], nodes scan available channels and determine occupied channels by comparing the Energy Detection (ED) with a threshold. Finally, nodes select one of the idle channels to continue their communications over that. In [8], a node measures the activity and signal strength of interference on each channel. Afterwards, it ranks the channels according to these two criteria. In [9], a theoretical channel ranking algorithm is proposed based on PDR estimation. The PDR estimate can be achieved if the interference activity and signal strength are known. The ranking error bounds for such estimation is also considered.

In [10], an adaptive channel allocation method is proposed in which interfered nodes switch to another channel until interference disappears. Nodes can detect the interference through the Clear Channel Assessment (CCA) procedure. Affected nodes switch back to the original channel upon they find interference has diminished. In [11], an adaptive channel hopping is presented in which a sink node gathers the link quality information from all nodes at network initialization period. The sink node sorts available channels based on aggregate link quality information. If interference happens on current channel, the sink node sends a hopping command to another channel from sorted channels. Another interference detection method based on RSSI value is presented in [12] in which nodes can switch to another channel if they encounter interference on the current channel. This scheme achieved up to 50% reduction in packet loss rate.

1.3 Contribution

Most of the interference avoidance schemes are only able to detect interference-free channels, and they may not be useful in indoor environments where WLANs have been widely deployed and all the channels suffer from interferences. In additions, channel ranking methods usually assume that received signal power from another node is constant over all available channels. Hence they estimate the channel condition only based on noise and interference characteristic. But this assumption cannot be satisfied in most of real environments since propagation of signal in different channels are quite different from each other. In [13], it is shown that there is a significant frequency selective fading in 2.4 GHz band. This fact shows that signal strength in each channel should be considered for channel estimation as well as the co-channel interference. This thesis proposes a new channel ranking method that predicts channel quality for each channel considering both received signal strength and interference. In this method, channels are sorted according to estimated PDR on channels. Furthermore, the accuracy of PDR estimation scheme is investigated in both emulated and real life wireless channel conditions and confirmed that the algorithm is effective to classify channels.

1.4 Objective and Methodology

Channel ranking enables WSNs to find the optimal channels in a shared spectrum. The performance of a link in a specific channel can be described by achievable PDR on it, hence the PDR is chosen as a metric for this channel ranking algorithm. The PDR on a link depends on Signal to Interference plus Noise Ratio (SINR) value at the receiver node and the characteristic of co-channel interference in the time domain. The PDR estimation is carried out at receiver node according to the received signal energy from transmitter node, and noise and interference characteristics obtained through spectrum measurements on each channel.

The PDR estimation algorithm can be utilized for channel ranking purpose if it is capable of predicting the achievable PDR on each channel with desired accuracy. The PDR estimation algorithm is implemented in wireless sensor nodes to observe its accuracy in different channel conditions and under various interference patterns. Different traffics are generated by changing the number of packets per second and the payload size of packets. Following channel conditions are considered and emulated with the aid of a channel emulator:

- Gaussian channel in which signal from transmitter node and interferer node do not face any fading
- Fading channel only for interferer link in which interferer link experiences fading while transmitter node operates over a constant link
- Multipath fading channel for both links in which signals from transmitter node and interferer fade in the channel independently

The proposed channel ranking method is also assessed in an office environment at the department of Communications and Networking, Aalto University to rank 16 channels in 2.4 GHz band under interference from Wireless LANs (WLANs). The office environment presents the real channel condition for a typical WSN deployment.

1.5 Thesis Outline

The remainder of this thesis is organized as follows: Section 2, briefly introduces the IEEE 802.15.4 and IEEE 802.11 standards, as well as the different coexistence methods of these standards to operate in the shared medium. Section 3, describes the design and implementation of test-bed, hardware and software components of the test-bed, and methodology of experiments. A mathematical model of packet error rate in existence of noise and interference, and the algorithm of PDR estimation in different channel conditions are described in Section 4. In Section 5, the performance of PDR estimation method in different scenarios and performance of channel ranking in a real environment are investigated. Finally, Section 6 concludes the thesis and suggests future works.

2 Overview of IEEE 802.15.4 and IEEE 802.11 Standards

This section reviews the architecture of the IEEE 802.15.4 and IEEE 802.11 standards, as this thesis focuses on providing the channel ranking algorithm for WSNs under interference from WLANs. Section 2.1 depicts the Physical (PHY) layer and Media Access Control (MAC) of IEEE 802.15.4 and Section 2.2 depicts the PHY and MAC layer of IEEE 802.11. Section 2.3 describes the existing coexistence mechanisms for IEEE 802.15.4 standard with other standards.

2.1 IEEE 802.15.4

The IEEE 802.15 Task Group 4 (TG4) was charted to investigate a fundamental solution for low data rate devices [14]. The emphasis was on low complexity and low power consumption architectures that provide low cost communication between devices for months to years without changing the batteries. The IEEE 802.15.4 standard was emerged in 2003 by defining PHY and MAC layers for Low-Rate Wireless Personal Area Networks (LR-WPANs) [15]. A Full-Function Device (FFD) and a Reduced-Function Device (RFD) are the two different device types that can participate in a LR-WPAN. The FFD can operate in three modes serving as: a personal area network (PAN) coordinator, a coordinator, or a device. An FFD can talk to RFDs or other FFDs, while an RFD can talk only to an FFD. The original IEEE 802.15.4-2003 standard was modified later and superseded by IEEE 802.15.4-2006 [16]. These standards are basis for the ZigBee [17], WirelessHART [3], ISA-SP100 [4], and MIWI [18] specifications, each of them adds extensions for upper layers that are not defined by IEEE 802.15.4 standard. The PHY is designed according to the international unlicensed frequency bands. These standards can be utilized for different applications like sensors, interactive toys, remote controls, home automations, industrial monitoring systems etc. The IPv6 over Low power Wireless Personal Area Networks (6LoWPAN) standard makes nodes reachable from outside the network and provides an infrastructure to realize Internet of Things (IoT) applications [19].

Section 2.1.1 describes the PHY layer of IEEE 802.15.4 standard, while Section 2.1.1 explains the MAC layer of IEEE 802.15.4.

2.1.1 Physical layer

The PHY provides services for PHY data and PHY management. The PHY is responsible for data transmission and reception, activation and deactivation of the radio transceiver, calculation of LQI for received packets, performing channel selection, execution of ED and CCA to access the medium [15]. The standard specifies three different frequency bands to be utilized by PHY. These bands are on 868 MHz, 915 MHz and 2.4 GHz and a compliant device should operate at least in one of them. Although these bands are allocated to ISM applications by Radiocommunication Sector of International Telecommunication Union (ITU-R), individual

countries may restrict to use some of these bands according to their national radio regulations [20]. For instance, the 915 MHz band in Europe and 868 MHz in North America are prohibited to be utilized by this technology.

The transmission schemes in all these frequency bands rely on Direct Sequence Spread Spectrum (DSSS) technique while different modulation techniques are adopted according to the operational frequency band. The initial IEEE 802.15.4-2003 standard specifies Binary Phase-Shift Keying (BPSK) modulation as PHY for 868 and 915 MHz bands which provide data rate up to 20 kbps and 40 kbps respectively. The revised IEEE 802.15.4-2006 standard suggests two other optional PHYs with more complexity for 868/915 MHz bands to provide higher data rates [16]. The first optional PHY utilizes Parallel Sequence Spread Spectrum (PSSS) with Amplitude Shift Keying (ASK) and provides 250 kbps data rate for data transmission. The other optional PHY employs Offset-Quadrature Phase shift Keying (O-QPSK) modulation and achievable data rate is 100 kbps for the 868 MHz band and 250 kbps for the 915 MHz band. The standard specifies O-QPSK modulation for well-known 2.4 GHz frequency band and maximum 250 kbps data rate can be achieved. The modulation schemes, spreading formats and achievable data rates of available PHYs are summarized in Figure 1.

PHY (MHz)	Frequency band (MHz)	Spreading parameters		Data parameters		
		Chip rate (kchip/s)	Modulation	Bit rate (kb/s)	Symbol rate (ksymbol/s)	symbols
868/915	686-686.6	300	BPSK	20	20	Binary
	902-928	600	BPSK	40	40	Binary
868/915 (optional)	686-686.6	400	ASK	250	12.5	20-bit PSSS
	902-928	1600	ASK	250	50	5-bit PSSS
868/915 (optional)	686-686.6	400	O-QPSK	100	25	16-ary Orthogonal
	902-928	1000	O-QPSK	250	62.5	16-ary Orthogonal
2450	2400-2483.5	2000	O-QPSK	250	62.5	16-ary Orthogonal

Figure 1: Frequency bands and data rates of IEEE 802.15.4 [16]

The IEEE 802.15.4 PHY offers a total of 27 channels in three available bands, one in the 868 MHz band, ten in the 915 MHz band, and 16 in the 2.4 GHz band. Channels are numbered from 0 to 26. List of channels and corresponding frequencies in 2.4 GHz band can be found in Appendix A. This thesis concentrates on sensor nodes that operate in 2.4 GHz band.

2.4 GHz PHY specifications: A 16-ary quasi-orthogonal modulation technique is utilized by the 2.4 GHz PHY where four data bits select one of 16 nearly orthogonal Pseudo Noise (PN) sequences to form one symbol. PHY employs O-QPSK to modulate carrier by the aggregated chip sequences derived from PN sequences of successive data symbols. In this PHY, chip rate is 2 Mchips/s and 250 kbps data rate is achievable. The procedure of modulation and spreading of bits to carrier is shown in Figure 2.

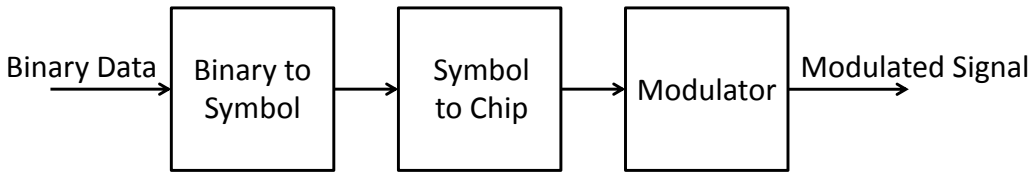

Figure 2: Modulation and spreading functions of IEEE 802.15.4 [16]

Regardless of their operational frequency band, all PHYs have following tasks in common:

Activation and deactivation of the radio transceiver: The PHY is responsible for turning on and off the radio transceiver pursuant to the MAC's request. PHY puts the radio in transmit (TX) mode when intends to send data and switches to receive (RX) mode to get incoming data. In order to reduce the power consumption, PHY puts the radio in sleep mode during idle time.

Channel selection: Each device should be able to work in one of the three available frequency bands. Each band has a subset of channels and each device can operate in a single channel at a time. The PHY shall change to desired channel upon request from upper layers.

Energy Detection (ED): The receiver ED tries to estimate the received signal power on the selected channel. This estimated energy can be used by MAC in order to execute the channel selection algorithm. The result should be reported as an 8-bit integer value ranging from 0x00 to 0xff. The ED is averaged and calculated over period of 8 symbols, i.e. 128 μs. The standard mentions that the minimum reported ED value should be within 10 dB above the receiver sensitivity and the difference between reported ED value and actual energy on the channel needs to be less than 6 dB. This procedure should be done without any attempt to identify or decode signals on the channel.

Link Quality Indicator (LQI): The LQI measurement shows the strength and/or quality of received packet. LQI can be calculated based on using received ED, Signal to Noise Ratio (SNR) estimation, or combination of these methods. PHY should calculate LQI for each received packet and report as an 8-bit integer to the MAC sublayer. LQI range is between 0x00 to 0xff which are corresponding to the lowest and highest quality that can be detected by the receiver respectively. The values for other qualities should be distributed uniformly within these two boundaries and at least eight distinct values should be used.

Clear Channel Assessment (CCA): The PHY employs CCA to identify whether channel is idle or busy. Before each packet transmission, CCA should be executed to make sure no device is currently transmitting on the channel. This mechanism reduces collision between packet transmissions and interference from other device and leads to better performance. The PHY should be able to implement at least one of the following three methods [16]:

- CCA Mode 1: Energy above threshold.
  CCA reports the channel as busy if received signal energy on it is above the threshold.
- CCA Mode 2: Carrier sense only.
  CCA tries to find a compliant signal with the PHY characteristics like modulation and spreading. Energy of such signal can be above or below the threshold level. In case of finding such signal, channel is considered as busy.
- CCA Mode 3: Carrier sense with energy above threshold.
  This mode is a logical combination of receiving energy above the threshold and receiving the signal compliant with PHY features. The logical operator can be set as AND or OR.

2.1.2 MAC sublayer

The MAC sublayer manages the access to the physical radio channel and handles the following task:

- Creating network beacon for coordinator node
- Synchronization of nodes to network beacons
- Handling Personal Area Network (PAN) association and disassociation
- Supporting security for nodes
- Executing the Carrier Sense Multiple Access with Collision Avoidance (CSMA/CA) to access to the channel
- Employing the Guaranteed Time Slot (GTS) mechanism
- Communicating with other peer MAC entity

Besides these responsibilities, the MAC sublayer also provides two services. The MAC data service transmits and receives the MAC protocol data along with the PHY data service. The MAC management service which acts as an interface to the MAC sublayer Management Entity (MLME) Service Access Point (SAP).

The standard defines two different types of channel access mechanisms based on the existence of beacon signal.

Non beacon-enabled mode: In the non beacon-enabled mode nodes employ an un-slotted CSMA/CA mechanism to access the channel upon the request of data transmission. In this mechanism, node performs the channel sensing after a random backoff period. If the channel is found idle the node transmits its data; otherwise it enters again in the backoff state. There exists a maximum number of time that node can try to access to the channel. When the maximum is reached, the algorithm ends and nodes tries to transmit another packet. In case that node transmits a packet successfully, the receiver node may transmit an optional acknowledgment (ACK) frame to inform the transmitter of successful reception.

Beacon-enabled mode: In the beacon-enabled network, a PAN coordinator node transmits a message periodically that is called beacon. The coordinator forms superframe structure which is bounded to consecutive beacons. All other nodes use the beacon signal to synchronize to the coordinator node and identify the PAN. Each node intends to transmit a data during the Contention Access Period (CAP) should compete with other nodes to access to the channel using slotted CSMA/CA mechanism. In a network with low traffic, the superframe can be divided into two parts: active period which is used for packet transmission and inactive period which nodes can enter a low-power mode to save energy. The coordinator node may also reserve a portion of active period as a Contention Free Period (CFP). These portions are called guaranteed time slots and devices requiring guaranteed Quality of Service (QoS) can transmit their data without any contention.

The standard designed the frame structures to avoid complexity and provide robustness against the noise. The MAC and PHY layers add headers and footers successively to the structure. The standard defines following frame structures: beacon frame, data frame, acknowledgment frame and MAC command frame.

Beacon frame: The beacon frame is used in beacon-enable PAN networks and transmitted by the coordinator node. The beacon frame is generated by the MAC sublayer and contains the superframe specifications, GTS fields, pending address fields, and beacon payload. The schematic view of the beacon frame is shown in Figure 3.

Data frame: Data generated in upper layers are passed to the MAC sublayer as data payload to be transmitted to other nodes. MAC sublayer adds MAC Header (MHR) as prefix and MAC Footer (MFR) as appendix to the MAC payload and

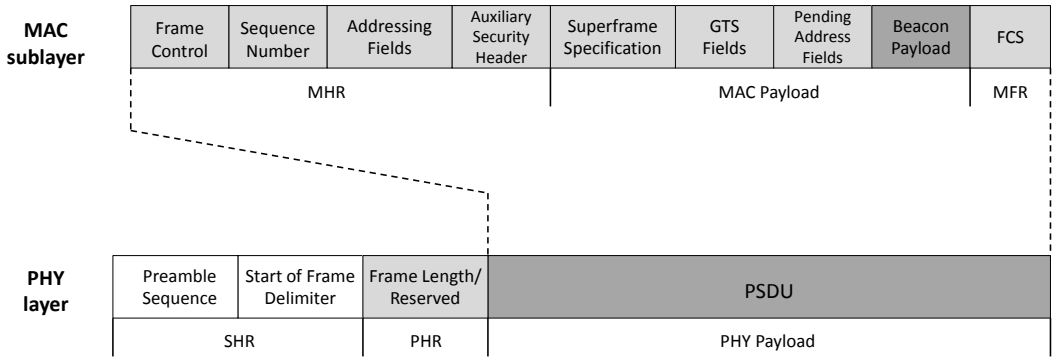

Figure 3: Schematic view of the beacon frame and the PHY packet [16]

delivers to the PHY as the Physical Service Data Unit (PSDU). Synchronization Header (SHR) and PHY Header (PHR) are appended to the PSDU and form the PHY packet. The procedure of forming PHY Protocol Data Unit (PPDU) from data payload is presented in Figure 4.

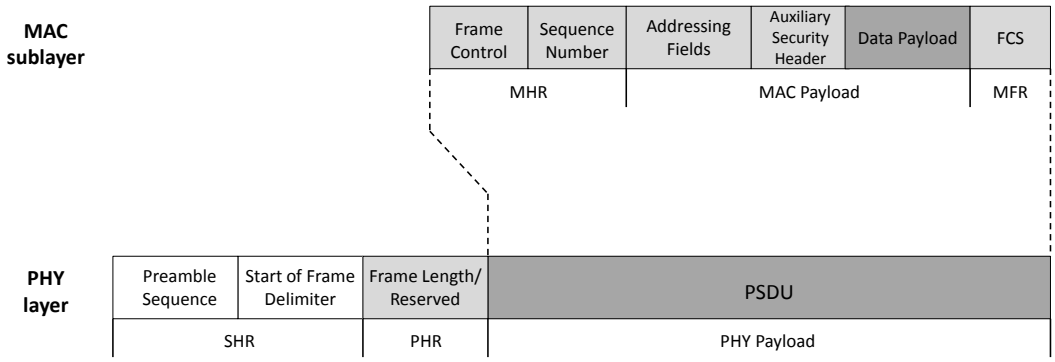

Figure 4: Schematic view of the data frame and the PHY packet [16]

Acknowledgment frame: The acknowledgment frame is generated by MAC sublayer to inform the transmitter node that packet has been received correctly. The MAC sublayer forms the acknowledgment frame with MHR and MFR without any MAC payload. The construction of acknowledgment is shown in Figure 5.

MAC command frame: The MAC command frame is originated from the MAC sublayer and used for network management and control. The MAC payload consists of command type and command payload. The frame structure can be seen in Figure 6.

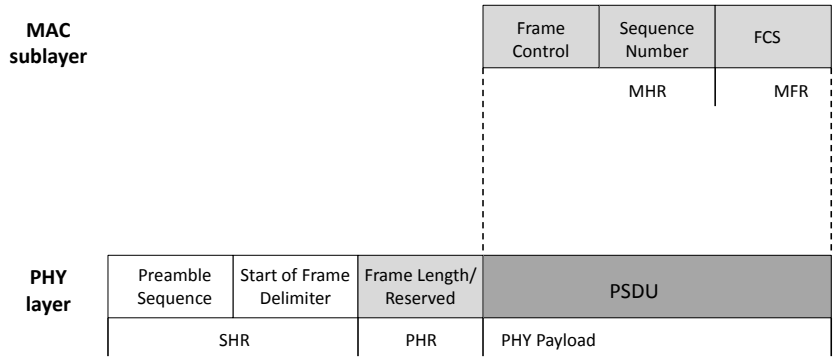

Figure 5: Schematic view of the acknowledgment frame and the PHY packet [16]

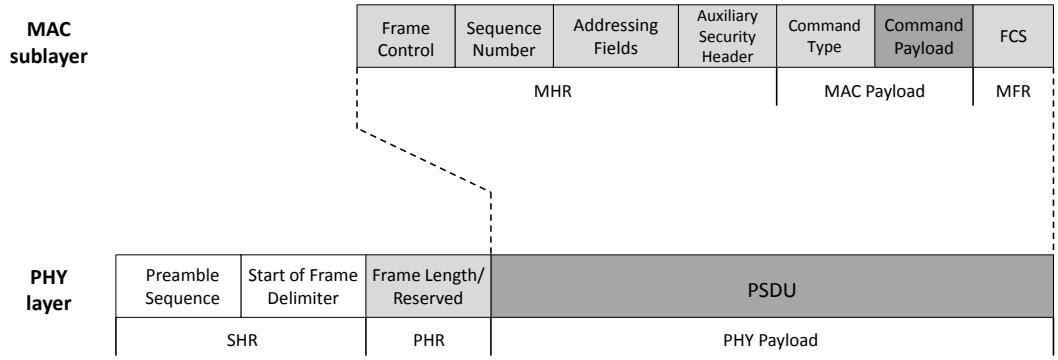

Figure 6: Schematic view of the MAC command frame and the PHY packet [16]

2.2 IEEE 802.11

IEEE 802.11 wireless networks have gained increasing popularity in recent years, providing users mobility and flexibility in accessing information. The IEEE 802.11 working group started to develop a standard for Local Area Networks (LANs) with wireless connectivity. Untethered, low cost, and high data rate communication are some of the reasons that this technology has become the dominant architecture in practice for accessing the Internet in offices, hotels, restaurants, etc. Nowadays most of the mobile phones, laptops and tablets are typically equipped with this technology. In demand of higher data rates, the standard has been revised many times and different versions have been released. These standards define PHY and MAC for WLANs. The PHY and MAC layers of the IEEE 802.11 standards are described in Section 2.2.1 and Section 2.2.2 respectively.

2.2.1 Physical layer

The original version of IEEE 802.11 standard was released in 1997 by introducing three alternative PHY technologies including DSSS, Frequency Hoping Spread Spectrum (FHSS) and diffuse Infrared (IR). All of those PHYs operate at either 1 or 2 Mbps. To meet the demand for higher data rate link connections, IEEE 802.11a introduces a PHY operating in 5 GHz frequency band employing Orthogonal Frequency Division Multiplexing (OFDM). An OFDM system achieves high spectral efficiency by dividing the whole available bandwidth into narrowband subcarriers, subsequently fading becomes almost flat with respect to the subcarriers. In 5 GHz band, the 22 MHz bandwidth is split into 52 subcarriers; 48 are used for data transmission and 4 are used as pilot. Data streams are transmitted simultaneously over subcarriers using BPSK, QPSK, 16-Quadrature Amplitude Modulation (QAM), or 64-QAM modulation. The OFDM scheme with punctured convolutional code provides a variable data transmission rate from 6 Mbps up to 54 Mbps.

IEEE 802.11b suggests two different modulations for original standard operating in 2.4 GHz band. The mandatory scheme is known as Complementary Code Keying (CCK), and an alternate is known as Packet Binary Convolutional Coding (PBCC). Both of these modulation methods support data rates of 5.5 and 11 Mbps. Higher operational frequency in IEEE 802.11a has the drawback of less coverage area compared to the IEEE 802.11b which operates in lower frequency band. To provide high-speed data rates, with wide-area coverage, IEEE 802.11g adds OFDM scheme as mandatory modulation for PHY in the 2.4 GHz along with two other optional modulation schemes. Although the OFDM system can provide data communication capabilities of 6, 9, 12, 18, 24, 36, 48, and 54 Mbps, supporting more than 24 Mbps is not mandatory. Currently, IEEE 802.11b and IEEE 802.11g are the most popular among proliferated standards, which are amendment to the original standard operating in 2.4 GHz band. Both of these standards define 14 channels in 2.4 GHz band, numbered 1 through 14. Channel separation is 5 MHz and each channel has 22 MHz bandwidth. Details of this channel mapping can be found in the channel frequency table in Appendix B.

The IEEE 802.11 Task Group next generation (TGn) in 2003 began to investigate the solutions that can achieve data throughput over 100 Mbit/s. This is accomplished by employing different improvements on the PHY as well as on the MAC [21]. Multiple-Input Multiple-Output (MIMO) antennas technique is implemented to take advantage of multi-path signal propagation. Another amendment in the PHY is bonding the channels which utilizes two non-overlapping channels simultaneously for transmission and provides 40 MHz operational bandwidth. Other modifications are done on MAC to intensify the efficiency, like bursting and aggregating frames and using compressed headers. Applying the frame aggregation allows the transmission of several payload packets within one channel access. Obviously, this improves the efficiency as the overhead for framing and channel access is only spent once [22].

2.2.2 MAC sublayer

The MAC sublayer of IEEE 802.11 provides communication for multiple nodes within a LAN or Metropolitan Area Network (MAN). Specifically, the MAC sublayer is responsible for the channel allocation procedure, Protocol Data Unit (PDU) addressing, frame formatting, error checking, and fragmentation and reassembly. The fundamental access method of IEEE 802.11 MAC is the Distributed Coordination Function (DCF) in which stations intend to transmit data, contend to access the channel. Point Coordination Function (PCF) is an optional mode relies on the Point Coordinator (PC) to poll frames from other stations. However, PCF wastes the channel bandwidth when stations with no data to transmit need to respond to a poll command by transmitting a null packet. For this reason, the PCF is not broadly used for commercial Access Points (APs). Request to Send/Clear to Send (RTS/CTS) is another optional method that can be implemented on top of the DCF to improve the performance of channel accessing by reserving the medium for a given frame. The IEEE 802.11 supports three different frames such: management frame, control frame, and data frame.

Some of the IEEE 802.11 MAC functionality can be described as:

DCF: The DCF is a MAC technique to access the medium based on the CSMA/CA protocol. The CSMA/CA is a wireless counterpart of Carrier Sense Multiple Access with Collision Detection (CSMA/CD) implemented for wired LAN. Collision Detection (CD) is not used in WLANs since transmitter node is not capable of listening to the channel to detect collision during its transmission. Receiver node transmits an ACK frame to the transmitter after each frame reception to inform that transmission was successful. Priority of different type of frames can be controlled by utilizing Interframe Space (IFS). The standard defines three different IFS intervals: Short IFS (SIFS), PCF Interframe Space (PIFS) and DCF Interframe Space (DIFS). Before stations try to access the channel, they should sense the channel to be idle. If a station senses that the channel is idle, it waits for a IFS period according to the packet type and after that, it checks the channel again. If the channel is still idle, station can access to the channel. For instance, ACK frame that has the smallest IFS, i.e. SIFS, is able to access the channel faster compared to the data frame. Process of accessing the channel is shown in Figure 7.

To reduce the collision probability in data transmissions from different stations, all stations should use a random backoff time before transmitting data frames. The backoff is a random integer value, uniformly distributed over the range 0 to so-called Contention Window (CW). Each station selects a backoff number before transmitting the data frame. When the medium becomes idle after a DIFS period, station countdowns the backoff timer to reach zero or channel become busy. The station freezes its timer on condition that the channel becomes busy. When the channel becomes idle again, station continues to countdown the backoff timer. Finally, station transmits the frame when the timer reaches to zero. If a collision occurs, station

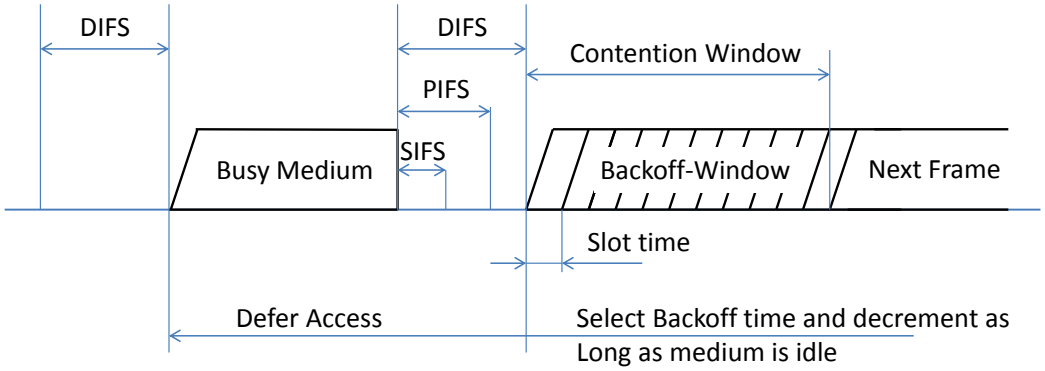

Figure 7: Basic access method of IEEE 802.11 [23]

should select another backoff number in a wider range and tries to retransmit the frame again. The value of contention window will be increased after each unsuccessful transmission until it reaches the maximum allowed value. The CW value for each transmission is within a range of $[CW_{min}, CW_{max}]$. The example values of CW for initial attempt and retransmissions of exponential increase in backoff window size are presented in Figure 8. Transmitter station waits to receive the ACK response from the receiver after transmitting a frame without collision. If transmitter receives the ACK, it transmits next frame, otherwise it retransmits the previous frame. The procedure of transmitting frame and ACK response is presented in Figure 9.

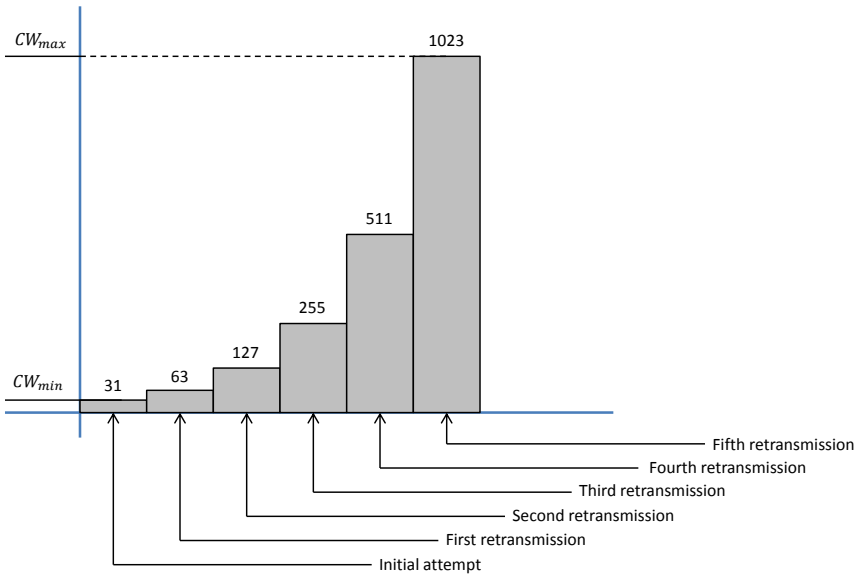

Figure 8: Example of exponential increase of CW [23]

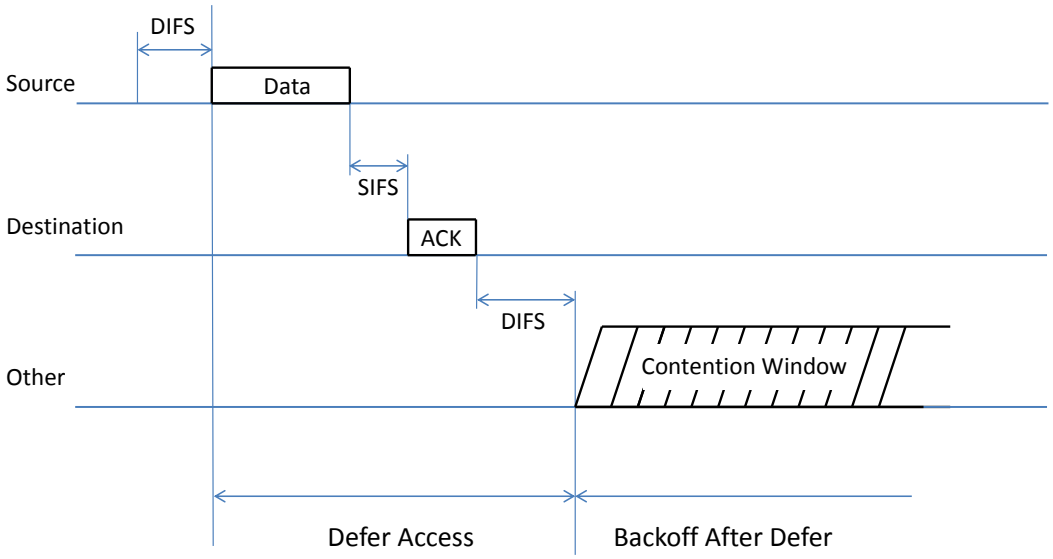

Figure 9: Individually addressed data/ ACK MPDU [23]

RTS/CTS: Since a source station is not capable of listening to the channel during its own transmission, it transmits the whole MAC Protocol Data Unit (MPDU) even if a collision happens. Collision mostly happens in the CSMA/CA mechanism because of hidden stations which are not in a range that able to sense the transmission of originating station. Accordingly, collision wastes a lot of scarce bandwidth specially when MPDU is large. Request to send (RTS), Clear to Send (CTS) control frames can be utilized to reserve the channel prior to the MPDU transmission and minimize the collision time. Source station transmits a RTS control frame before the MPDU and informs the destination about the duration of MPDU intended to be transmitted. Other stations that hear this message read the duration field and set their Network Allocation Vector (NAV) accordingly. NAV indicates amount of time that station must wait until ongoing transmission session is finished. Destination station responds the RTS with CTS immediately after a SIFS period. Stations that hear the CTS message, including hidden stations from source station, read the duration field and update their NAV. Source station starts to transmit MPDU upon successful reception of CTS on a reserved medium. Other stations can contend to access to the channel after destination station transmits a ACK message. The mechanism of transmitting an MPDU using the RTS/CTS is illustrated in Figure 10.

2.3 Coexistence of IEEE 802.15.4 with other Standards

Since the usage of ISM bands increases with emerging new applications and technologies, some techniques are required to assure multiple standards can coexist in the shared medium. The IEEE P1900 Standards Committee was established in 2005

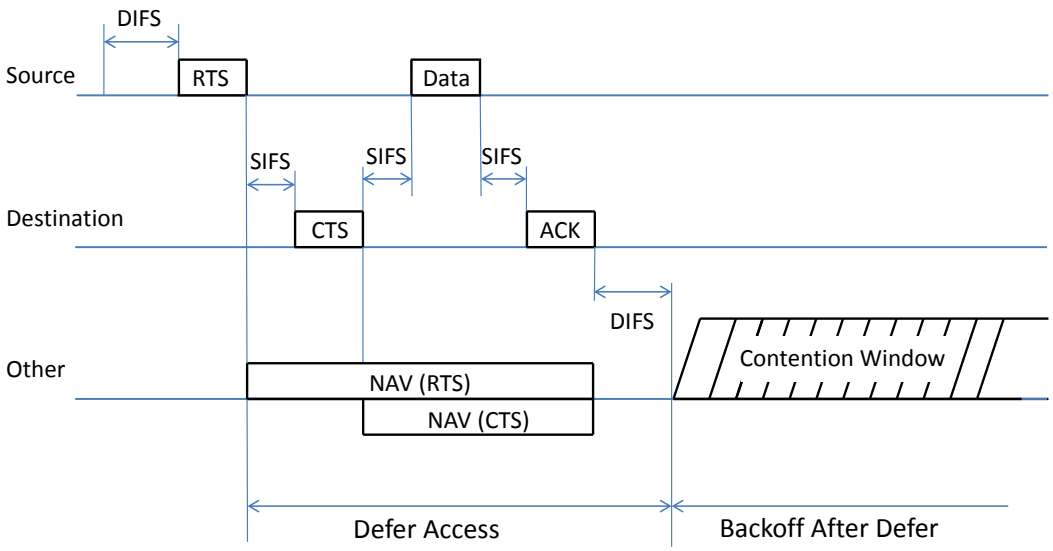

Figure 10: RTS/CTS/data/ACK and NAV procedure [23]

to develop supporting standards dealing with new technologies and techniques being developed for next generation radio and advanced spectrum management [24]. The committee is divided in subcommittees and concentrates on various solutions for harmonized cohabitation of multiple existing and evolving heterogeneous wireless radio standards [25]. More precisely, the IEEE 802.19 coexistence Technical Advisory Group (TAG) was formed to deal with coexistence issues of wireless networks working under development within IEEE 802 in unlicensed frequency bands. Earlier, the IEEE 802.15 coexistence Task Group 2 (TG2) developed a set of mechanisms to facilitate coexistence of Wireless Personal Area Networks (WPAN) and WLAN [26]. These methods can be classified as collaborative or non-collaborative mechanisms. The collaborative techniques can be employed to reduce the mutual interference if competitive standards are capable of exchanging information between one another. For instance, in the beacon enabled mode for IEEE 802.11, access point transmits beacon packets periodically. The beacon-to-beacon interval can be divided into two subintervals: one for the IEEE 802.11 traffic and one for the IEEE 802.15.4 traffic. However, to bring this method into existence, a dedicated communication link is required to synchronize networks with each other. Non-collaborative techniques can be employed where competitive technologies operate independently. These methods rely on capability of the IEEE 802.15.4 MAC to detect and distinguish any type of interference or jamming in the system and adapt its operation to the vicinity. The IEEE 802.15.4 standard provides several mechanisms that facilitate the coexistence of WSNs with other wireless devices operating in the same spectrum. This section provides an overview of the mechanisms that are defined in the standard.

2.3.1 Clear Channel Assessment (CCA)

The IEEE 802.15.4 PHY performs CCA for the CSMA/CA mechanism to access the channel. It was mentioned in section 2.1.1 that PHY employs ED over a certain threshold, detection of compliant signal with IEEE 802.15.4 standard, or combination of both of them to assess the clear channel. Use of the ED option allows transmission backoff if another device with any communication protocol occupies the channel. As a result, the coexistence performance with other standards will be increased.

2.3.2 Modulation

The IEEE 802.15.4 PHY in 2.4 GHz band spreads the symbols with nearly orthogonal PN sequences. This power-efficient modulation method requires low SINR at the expense of using wider signal bandwidth compared to symbol rate. Typical low cost detectors need 5 or 6 dB SNR to work with less than 1% Packet Error Rate (PER). The interference from wide band systems like IEEE 802.11 impacts on IEEE 802.15.4 receivers like white noise. The IEEE 802.11 operational bandwidth is much wider than IEEE 802.15.4 bandwidth; hence it only injects a small portion of power to overlapped IEEE 802.15.4 channels. It is shown in [27] that around 17% of transmitted power from IEEE 802.11 falls within the IEEE 802.15.4 nearest central frequency channel. As a result, performance of the detector in existence of such interference is similar to the performance of white noise, but the overall required Signal to Interference Ratio (SIR) is 9 to 10 dB lower. On the other hand, interference from IEEE 802.15.4 appears as narrow band interference to IEEE 802.11 receivers. However, the spread spectrum technique in IEEE 802.11 moderates the interference effects from IEEE 802.15.4.

2.3.3 Low duty cycle and low transmit power

The IEEE 802.15.4 standard provides specifications for low power and low data rates applications. It is expected that these applications run at duty cycle of less than 1%. Although wireless devices are allowed to transmit data with power up to 1 W in the 2.4 GHz band, the majority of IEEE 802.15.4 devices operate with transmittion power between -3 dBm and 10 dBm to overcome their power constraint. These two features ensure that operation of IEEE 802.15.4 devices will not cause any noticibale interference on other collocated devices.

2.3.4 Channel alignment

A common channel allocation for the IEEE 802.15.4 in 2.4 GHz band is accepted globally and 16 channels are defined in this band. The IEEE 802.11 defines 14 channels in this band, however, channel usage depends on the regulatory domain. For instance channels 13 and 14 are prohibited to be used by WLANs in the US and Canada. This allows that the IEEE 802.15.4 nodes operate on channels 25 and 26 without interference from IEEE 802.11 devices. In addition, the IEEE 802.11

standard recommends that WLANs use one of non-overlapping channels; channels 1, 6 and 11 are suggested for North America, and channels 1, 7 and 13 for Europe. The suggested channels are shown in Figure 11 along with IEEE 802.15.4 channels. Although using non-overlapping channels is not mandatory, following this operating practice provides further clear channels for operation of IEEE 802.15.4 [28]. Nevertheless, utilizing these channels may be delicate since the IEEE 802.11 nodes may work on different channels than the recommended ones or might utilize dynamic channel allocation.

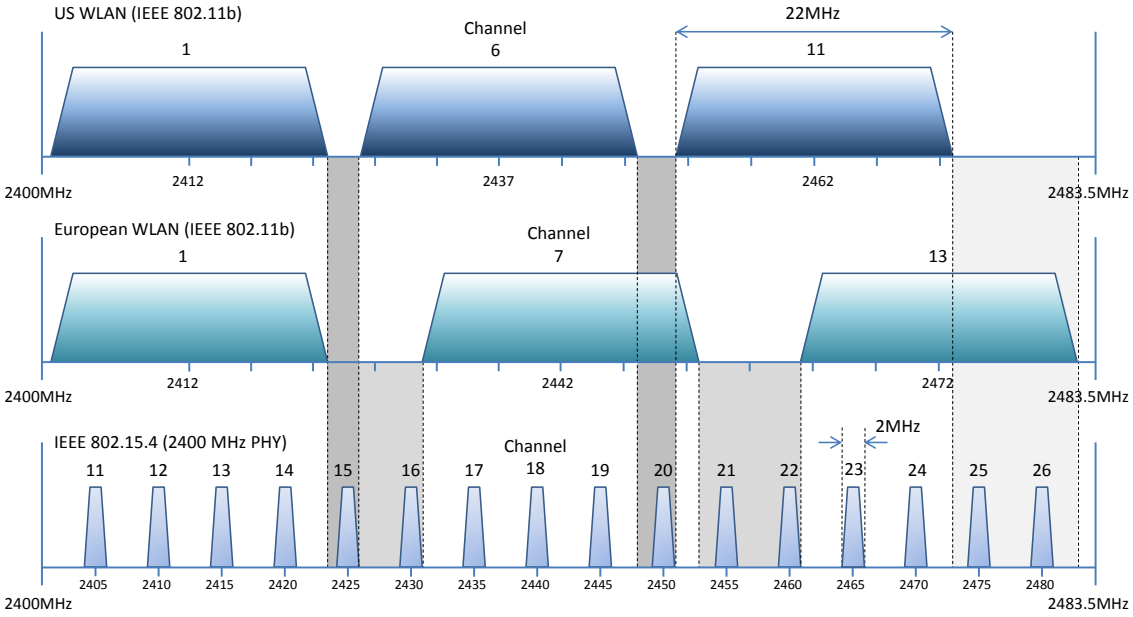

Figure 11: IEEE 802.15.4 (2.4 GHz PHY) channels vs. non-overlapping IEEE 802.11 channel allocations [29]

2.3.5 Dynamic channel selection

The IEEE 802.15.4 standard defines dynamic channel selection scheme. At network initialization or in case of outage, the IEEE 802.15.4 devices scan the set of predefined channels. This feature allows that IEEE 802.15.4 devices choose another channel if a current channel is occupied by another network.

2.3.6 Neighbor piconet capability

Although the IEEE 802.15.4 standard does not specify interoperability with other systems, this feature can be used to reserve a portion of time for communication of this network. This capability needs cooperation between different systems and alleviates interference between competitive systems.

3 Design and Implementation of the Test-Bed

This section describes the design and implementation of test setup for the performance measurement of PDR estimation algorithm. Several experiments are carried out to observe the PDR performance under various interference conditions and propagation channels. The design and implementation of experimental setups are presented in Section 3.1, while hardware and software elements of IEEE 802.15.4 nodes and interferer node are introduced in detail in Section 3.2 and Section 3.3 respectively. Section 3.4 presents the behavior of the wireless channels and different channel models used to emulate various wireless conditions. Finally, the experimental methodology is presented in Section 3.5.

3.1 Test-Bed Design and Implementation

The test-bed is implemented in Communications lab at the department of Communications and Networking, Aalto University. The Experimental tests are carried out in three different setups which model different channel conditions.

- *Wired channel:* This setup is prepared to remove the effects of fading in the channel. Both signals from IEEE 802.15.4 and IEEE 802.11 pass through constant channels. Details of this setup described in Section 3.1.1.
- *Fading channel for IEEE 802.11 link connection:* In this setup only IEEE 802.11 link experiences fading, while communication of IEEE 802.15.4 nodes is over the Gaussian channel. Section 3.1.2 presents more details about this setup.
- *Fading channels for both IEEE 802.11 and 802.15.4 link connection:* This setup provides more realistic channel condition in which both signals from IEEE 802.15.4 and IEEE 802.11 undergo independent fading in the channels. The detailed setup is presented in Section 3.1.3

3.1.1 Wired channel setup

Wired setup is used to evaluate the performance of PDR estimation for IEEE 802.15.4 packet transmissions in the presence of interference from IEEE 802.11 node in a constant propagation environment. The IEEE 802.15.4 platform is equipped with a module mounted chip antenna by default. To establish a wired connection, the mounted chip antenna is broken off and a micro-miniature coaxial connector (MMCX) is mounted for each node. An RF cable is connected to the MMCX connector of transmitter node to carry the signal energy to a circulator and then to an attenuator. IEEE 802.11 card has a Sub Miniature version A (SMA) connector which can be connected to the external antenna. An RF cable is connected to the SMA connector and signal energy from IEEE 802.11 node is passed through a circulator and the attenuator. Output signals from attenuators are combined together with the aid of a combiner and connected to the receiver node. Attenuators are used to control the signal amplitudes from IEEE 802.15.4 transmitter node and

IEEE 802.11 node. Circulators isolate the IEEE 802.11 and IEEE 802.15.4 transmitter nodes from each other and also from ambient co-channel interference. In this way, the IEEE 802.15.4 and IEEE 802.11 interferer nodes sense the channel idle whenever they want to access to the it. In the other words, interferer node does not affect the IEEE 802.15.4 transmitter and only disturbs the receiver node by introducing interference. The complete setup is shown in Figure 12 .

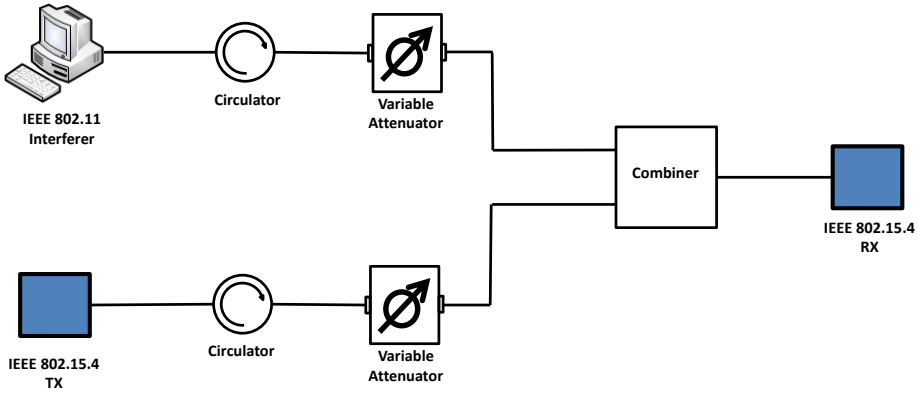

Figure 12: Wired connection test-bed diagram

3.1.2 Fading channel for IEEE 802.11

This setup is established to observe the performance of PDR estimation for packet transmissions between IEEE 802.15.4 nodes in which the signal energy from transmitter node is passed through a constant link connection, while signal from interferer faces fading in the channel. This scenario may happen in real environments that sensor nodes are placed near to each other and a strong LOS propagation path exists among them. In order to provide this condition, signal strength from transmitter node is kept fixed by connecting the node through the wired connection and signal from interferer is passed through a channel emulator. Output signal from the channel emulator is combined with transmitter node signal and delivered to the receiver node. Different channel models can be used to model various fading channels for interferer link. The complete setup is shown in Figure 13.

3.1.3 Fading channel for IEEE 802.11 and IEEE 802.15.4

In this setup, a complicated model is considered in which both the IEEE 802.15.4 and IEEE 802.11 links experience fading. This is a more realistic scenario which models wireless channel in real environments. In this setup, both signals from IEEE 802.15.4 and IEEE 802.11 are subjected to fading through two independent emulated channels. Faded signals are combined together and are handled with receiver node. Since signals from IEEE 802.11 and IEEE 802.15.4 nodes are passed through two

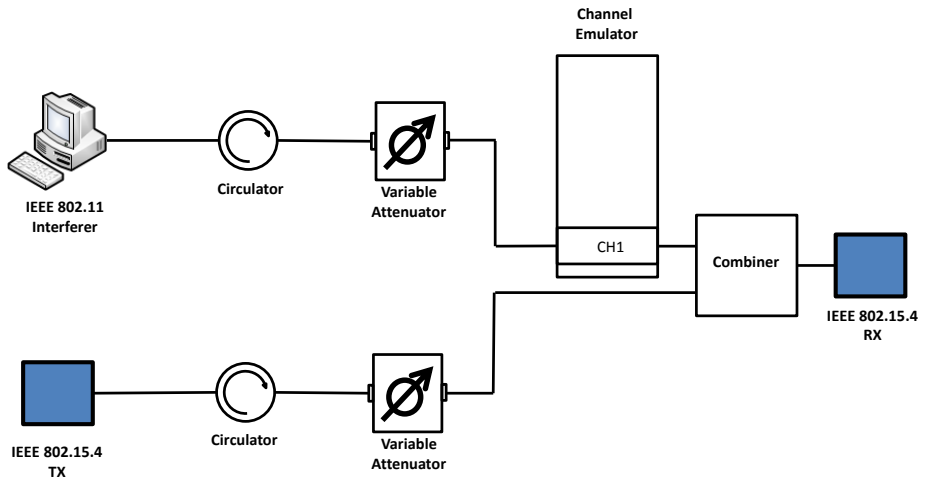

Figure 13: Test-bed diagram of fading channel for IEEE 802.11 link

separated channels, independent channel models can be defined for each link. The complete setup is shown in Figure 14.

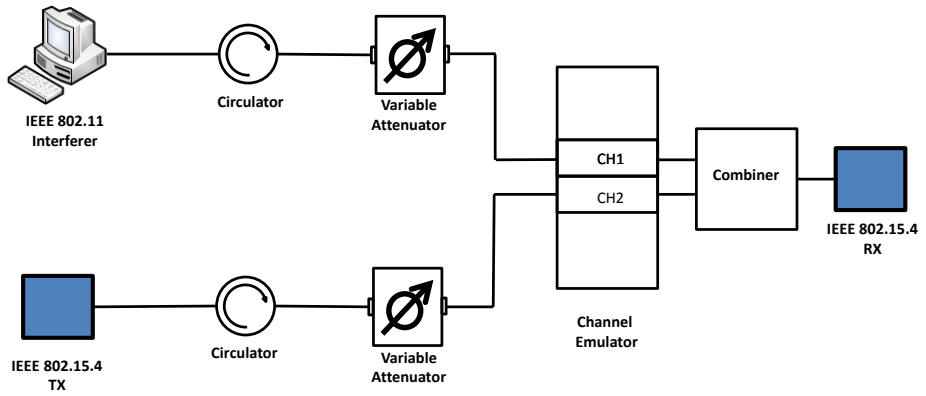

Figure 14: Test-bed diagram of fading channel for IEEE 802.11 and IEEE 802.15.4 link connections

3.2 IEEE 802.15.4 Node

In order to establish a IEEE 802.15.4 wireless sensor link, micro-series nodes provided by Sensinode are used in experiments [30]. Sensinode developed U100Micro2420 node as a FFD. This platform is integrated with a low power Texas Instrument MSP430 micro controller (μC) and a Chipcon CC2420 as transceiver radio that is compliant with IEEE 802.15.4 standard [31]. An external Flash memory with 4 MB capacity is connected to MSP430 through the serial port interface, which can be

used to store collected data. A Complex Programmable Logic Device (CPLD) connects the Micro2420 modules together and generates reset, clock and select signals for elements. Two AAA batteries with minimum voltage of 1.5 V power the Micro2420 platform. Additional sensors can be connected to the platform through two external connectors. A real-time open source operating system, FreeRTOS, manages hardware resources in this platform. Sensinode developed a communication stack, i.e. NanoStack which is an open source 6LowPAN protocol and provides an IEEE 802.15.4 MAC and communication protocols and runs on top of FreeRTOS operating system.

3.2.1 MSP430

A programmable Micro Controller Unit (MCU) performs tasks, computes data and controls other peripherals of the wireless sensor platform. The MSP430 has been designed based on 16-bit Reduced Instruction Set Computer (RISC) and mixed-signal Central Processing Unit (CPU) [32]. Due to low cost and low power consumption of this micro controller family, this MCU is widely deployed in variety of wireless sensor platforms. The Micro2420 is equipped with MSP430F1611IRTDT that provides 48 KB Flash, 10240B Random Access Memory (RAM), 16-bit timers, 12-bit Analog to Digital Converter (ADC), Dual 12-bit Digital to Analog Converter (DAC), and two serial communication interfaces that provide Universal Asynchronous Receiver/Transmitter (UART) and I2C interface. The MSP430 works with low supply power in range of 1.8 V to 3.6 V. Five software configurable low power modes of operation are available which can be selected according to the node's task in order to minimize the power consumption. Current consumption can be reduced from 330 μA in active mode to 1.1 μA in standby mode, or 0.2 μA in off mode.

3.2.2 CC2420

The Chipcon CC2420 is a low power and low voltage transceiver operates in the 2.4 GHz unlicensed ISM band. This transceiver employs DSSS baseband modem that provides 9 dB spreading gain with effective rate of 250 kbps. The CC2420 is compliant with IEEE 802.15.4 and ZigBee systems [31]. The CC2420 PHY layer provides an 8-bit integer value known as the RSSI. The RSSI is an estimate of received signal power measured by radio and reported in dBm scale, in one dBm increment. Although reported RSSI value by CC2420 is linear, it may be different from actual received energy up to 6 dB. RSSI value is always averaged over 8 radio symbol periods, i.e. 128 μs. RSSI measurements can be categorized into two different types. The first category measures the signal strength of received packet from another IEEE 802.15.4 node, while the second measures the strength of the ambient channel noise and interference. To distinguish between these two different RSSI categories, they can be called as signal RSSI, and noise and interference RSSI respectively [33]. In addition to RSSI, CC2420 provides another 8-bit value called LQI which indicates measurement of chip error rate. The LQI is calculated by averaging correlation value of the 8 first symbols of header for each received packet and reported in a range of 0 through 255.

Some of the other important features of this chip are:

- DSSS transceiver with 2 MChips/s and 250 kbps effective data rate
- Suitable for both RFD and FFD
- Low current consumption with 18.8 mA for RX and 17.4 mA for TX
- Low supply voltage (2.1-3.6 V) with integrated voltage regulator
- Low supply voltage (1.6-2.0 V) with external voltage regulator
- No external RF switch / filter needed
- 8 programmable output power
- High sensitivity (-95 dB)
- Digital RSSI / LQI support
- Clear channel assessment
- O-QPSK with half sine pulse shaping modulation

3.2.3 NanoStack

Sensinode designed NanoStack as a communication stack, implements full 6LoWPAN architecture and IEEE 802.15.4 standard. It includes 6LoWPAN and User Datagram Protocol (UDP) implementations, Internet Control Message Protocol (ICMP), the IEEE 802.15.4 MAC and Simple Sensor Interface (SSI) sensor protocol. NanoMesh provides automatic multihop capabilities for NanoStack, using multihop forwarding protocol. Custom protocols can be defined for NanoStack as protocol elements. The stack and its protocol elements are built upon FreeRTOS, a stable and portable real-time operating system. Data communication is provided for applications through a socket interface which is widely implemented in Portable Operating System Interface (POSIX) compliant system. The NanoStack Application Programming Interface (API) follows the POSIX API, while adds memory management features to facilitate buffer operations [35]. The FreeRTOS schedules tasks and runs them in a sequential manner, i.e. a single task is proceeding at a time. This feature results in reduction of RAM usage and supporting effective flow control. The NanoStack is executed in the FreeRTOS environment as a single task loop and is responsible for module handler execution. Stack usage is more simplified by restricting the modules to call other functions directly. Supporting a single buffer queue ensures that user applications work smoothly and not blocked during protocol stack operation. The architecture of NanoStack is presented in Figure 15.

3.2.4 FreeRTOS

FreeRTOS is a free open source real time kernel which is designed for small embedded systems [34]. As the base of FreeRTOS is small and predominantly written in standard C, it can easily be ported to different hardware architectures. Complicated programs can be partitioned into smaller tasks and each task should be assigned

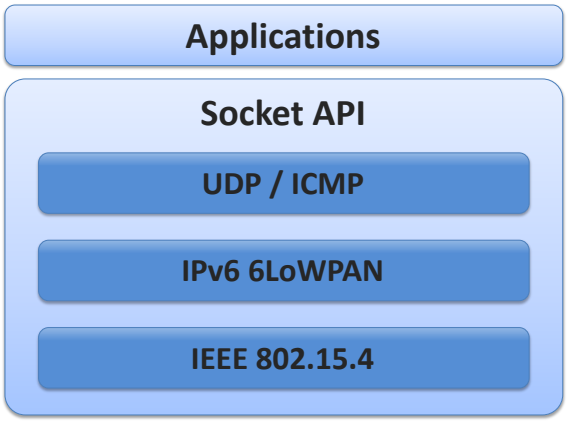

Figure 15: The NanoStack architecture [35]

with a priority. Since kernel of FreeRTOS has a priority-base scheduler, it shares the CPU between all tasks based on their priority and tasks with the same priority use the CPU in a Round Robin manner. The scheduler is capable of running tasks in preemptive, cooperative and hybrid modes. Tasks can communicate with each other through message queues and binary semaphores. By use of scheduling and inter-task communication, FreeRTOS can switch between different tasks and run them apparently concurrent. The behavior of multitasking in FreeRTOS is shown in Figure 16.

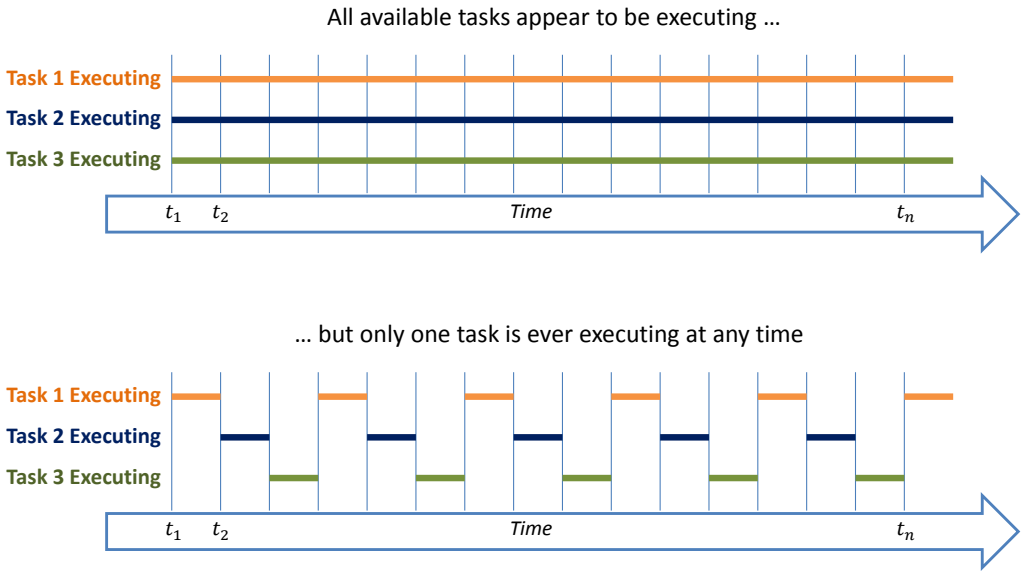

Figure 16: Multitasking behaviour of FreeRTOS [34]

The kernel suspends the running task when assigned time of that is over and resumes another task. This procedure happens sequentially and a task does not aware when it is going to get suspended or resumed by the kernel. Since all tasks utilize the same common processor resources, modifying the microcontroller registers by running task, may cause problems when other suspended tasks are resumed again. To avoid this problem, the kernel stores the context of each suspended task and restores data before it resumes the task again.

3.3 Interferer

A PC equipped with a wireless networking adapter is used to generate IEEE 802.11g signal as a source of interference. The PC is running Linux Ubuntu 10.04 and equipped with TP-Link TL-WN651G Peripheral Component Interconnect (PCI) adapter that supports IEEE 802.11b and IEEE 802.11g standards [36]. The radio module of this adapter is Atheros chipset that is supported by MadWifi drivers [37]. The Multi-Generator (MGEN) version 5.0 is installed and used to generate UDP traffics for wireless adapter [38].

3.3.1 MadWifi

The MadWifi is an abbreviation for multiband Atheros driver for wireless fidelity. This open source driver is developed for WLAN devices with Atheros chipsets [39]. By using this driver on Linux, the wireless device appears as a normal network interface in the system. Although the latest stable version of MadWifi is v0.9.4, the older MadWifi v0.8.2 is utilized. This is because in the latest driver version, Power Control Management (PCM) is enabled by default. This feature leads that output signal from the adapter changes. However, PCM in MadWifi v0.8.2 is disabled and signal output from adapter has a constant level.

3.3.2 MGEN

The Multi-Generator (MGEN) is an open source software that is capable of generating UDP, Transmission Control Protocol (TCP) and Internet Protocol (IP) traffics with different patterns [38]. MGEN can be used for different purposes like evaluating the performance of the IP networks or generating traffics for simulation environments like NS-2 and OPNET. By using script files, network can be loaded with different real-time traffic patterns. These script files can be used to emulate traffic patterns of unicast and/or multicast UDP and TCP/IP packets. Supported traffic patterns in this program are periodic, Poisson and burst. With periodic pattern, packets are generated with a constant inter arrival time, while inter arrival times of packets in Poisson pattern varies but the average number of transmitted packets remains constant. Burst traffic pattern models traffic from Voice Over IP (VoIP) applications in which a user starts to talk randomly (talk spurts) with some average inter arrival and duration of each spurt is exponentially distributed. It should be considered that MGEN generates traffic on application layer and it does not mean that PHY transmits packets with the same pattern. For instance, if the generated

traffic by MGEN is introduced to the IEEE 802.11 card and CCA is enabled, packets are transmitted when the channel is sensed idle by MAC.

3.4 Wireless Channels

The wireless channels by nature are variable and time-dependent. They are not stationary and predictable like wired channels, so analysis of them is more convoluted. An overview of the characteristics of wireless propagation is given Section 3.4.1. In order to simulate the wireless channel conditions in experiments, a channel emulator is used. Section 3.4.2 introduces the channel emulator and how it should be configured. Section 3.4.3 presents various channel models which are used in experiments to emulate different wireless propagation environments.

3.4.1 Wireless channel characteristics

The wireless channel model can be utilized to predict the mean received signal energy for an arbitrary transmitter-receiver separation which is helpful to estimate the radio coverage area. The mechanisms of electromagnetic wave propagation are diverse, but can generally be characterized in three mutually independent phenomena as: large-scale path loss, shadow fading and multipath fading.

- Large-scale path loss: The large-scale path loss is a function of distance between transmitter and receiver, and the materials that electromagnetic waves propagate through. Due to large-scale path loss, the received power varies gradually determined by the geometry of environment.
- Shadow fading: For a given path loss, there is a variation in received signal power over time which is referred as "shadow fading" or "slow fading". This may happen because of the changes in the environment, like people movements.
- Multipath fading: Usually signal offered to the receiver comes from different paths. Signals from multipath can be combined destructively or constructively according to their phases. Movements in the environment can change the situation of paths, and consequently influences on the received signal energy.

For a fixed transmitter and receiver, the large-scale path loss is a constant value. But two shadow fading and multipath fading should be considered in environments where elements may move.

3.4.2 Channel emulator

The EB Propsim C8 is an eight channel wideband radio channel emulator that can be used for modeling miscellaneous channel propagation models [40]. This channel emulator supports signal with maximum bandwidth up to 100 MHz frequency in frequency band from 350 MHz up to 6 GHz, therefore it can emulate wireless channels for large variety of wireless devices including IEEE 802.11 and also IEEE 802.15.4. The EB Propsim C8 first demodulates the original signal to the Analog

Baseband (ABB), filters and quantizes to digital values by ADC. Digital Signal Processing (DSP) part in emulator applies the effects of multipath fading by summing multipath parts to the Digital Baseband (DBB). Result signal is converted back to analog base band signal by DAC and eventually modulated to the initial RF. Because of this architecture of the EB Propsim C8, input and output of channels are completely isolated from each other and each channel should be utilized for one unidirectional connection.

Introducing different channel models to the EB Propsim C8 is possible by using Tapped Delay Line (TDL) by setting delays, average power and fading type for each tap. Up to 16 channels can be defined for this emulator and each channel supports 48 fading paths. A new channel model can be introduced for emulator in the channel model editor panel through Graphical User Interface (GUI). Average input level of signal, and crest factor which indicates the ratio between peak and average of the input signal should be set for the emulator in the same panel. Crest factor determines the quantization level of ADC and if it has not been set properly, it may cause saturation in the output of the signal and parts of the signal with high amplitude will be cut off. Average input level and crest factor can also automatically be set by Automatic Input Level Setting (AILS) when input signal is applied to the emulator. The output gain amplifies or attenuates the output signal to achieve a signal with proper amplitude. Mobile speed is another parameter that should be set and is inversely proportional to the coherence time of the channel. Higher value for this parameter causes that channel condition changes much faster during the simulation time. Central frequency of input signal should be entered in simulator editor panel. Finally, the model can be created and run by emulator from simulator control panel.

3.4.3 Channel models

The EB Propsim C8 gives possibility to emulate various wireless channels in a repeatable manner. Channel models can be used to emulate various channel conditions. Medbo and P.Schramn proposed different channel propagation models for Single-input Single-output (SISO) WLAN devices in different environments [41]. Medbo channel models are developed for some other environments and also for MIMO systems by the 802.11 Task Group n [42]. These models are applicable in both 2 GHz and 5 GHz frequency bands. Channel models are described based on delay time, distribution of amplitude and mean amplitude for each tap. Subsequent channel models are used as propagation models in our test-bed for IEEE 802.11 and IEEE 802.15.4 links:

- *Channel Model A:* Model A is applicable for typical office environment, Non-Line-of-Sight (NLOS) condition with 50 ns rms delay spread.

- *Channel Model D:* Model D is applicable for large open space (indoor and outdoor), Line-of-sight (LOS) condition with 140 ns rms delay spread. A spike of

10 dB Rican K-factor exists for first tap delay. The Rice factor K is the power ratio between LOS and NLOS components.

- *TGn Channel Model B:* TGn model B is applicable for smaller environments like residential homes and small offices with 15 ns rms delay spread.

The power delay profile for the channel models can be found in the Appendix C. The delay profile for each model consist of tap delays and their corresponding powers.

3.5 Experimental Methodology

It is desired to evaluate the capability of PDR estimation for channel ranking purpose under different interference and channel conditions. The performance of channel ranking is mainly determined by the accuracy of the PDR estimation algorithm on each channel. Hence in the rest of this thesis, we investigate the accuracy of PDR estimation method in a single channel. Obviously, if the PDR estimator satisfies desired accuracy under different interference conditions and various channel conditions, the estimation procedure can be repeated for other channels. Finally, channels can be ranked according to achieved PDR estimates on channels. The PDR estimation is carried out at receiver node by performing channel scanning to identify noise and interference characteristics. Then PDR is predicted for different received signal strength levels from the transmitter node. The accuracy of PDR estimation method is evaluated by comparing the estimation results with achieved PDR obtained from packet transmissions through the channel.

In order to achieve various interference conditions, originated from IEEE 802.11 node, different traffic patterns are generated. Interference can be varied either by changing the interference strength or by changing the interference activity. The Interferer node generated different UDP traffics by using MGEN program. Different traffic patterns are generated by varying packet rate and packet payload size of interferer. UDP traffic is used because it is the simplest type of IP traffic and ACK is not defined at higher layers. As a consequence, packet retransmission might not happen in UDP traffic in case of packet drop. In fact by using UDP traffic, we ensure that generated traffic on PHY has the same pattern as the generated traffic on application layer by MGEN. The IEEE 802.11 interferer is set to work in IEEE 802.11g mode and transmits packets in multicast mode at 11 Mbps.

In all experiments, IEEE 802.15.4 nodes employ CCA mode 2. In this mode, a node senses the channel occupied only if it finds transmission from another compliant device. This mode is employed to examine the worst scenario in which a sensor node may transmit data even it finds that the IEEE 802.11 interferer is transmitting on the channel. The IEEE 802.15.4 nodes operate at channel 22 with a center frequency of 2.46 GHz, while the IEEE 802.11 interferer operates at channel 10 with

center frequency of 2.457 GHz. The offset between center frequencies is 3 MHz.

In order to obtain the empirical achievable PDR, the IEEE 802.15.4 transmitter node sends packets in a broadcast mode every 30 ms. Payload size of packets is 24 bytes and the total packet size including the headers is 62 bytes. Transmitter node is capable of sending data at rate of 250 kbps, hence packet transmission time for each one of them is 1984 μs.

In order to evaluate the accuracy of PDR estimation algorithm for each interference condition, following steps are followed:

1. Receiver node scans and collects noise and interference RSSI samples from the channel. Collected samples are sent to the computer to perform PDR estimation for different signal strength levels from transmitter node.

2. To compare the results from estimation method with empirical PDR, the transmitter node sends 1000 packets. The receiver node counts the number of successful received packets and calculates the achievable PDR. The receiver node also records the signal RSSI values for received packets and reports the average of them as mean received signal strength. The quite high number of packets in each transmission ensures that the calculated PDR indicates the average achievable PDR in the channel under the interference condition, and does not represent the transient achievable PDR during a specific time interval.

3. After reception of each packet, the receiver node scans the channel and collects noise and interference RSSI samples from channel. Each RSSI sample is compared with a threshold to ensure that sample is from the interference. The of mean RSSI values is calculated for interference samples.

4. The receiver node reports the achieved PDR, mean RSSI for received packets and mean RSSI from interference to the computer.

These steps are repeated for different signal strength levels from the transmitter node to obtain the PDR ranging from 0 to 100% while the channel and traffic conditions are kept fixed.

4 Channel Ranking Method

As described in detail manner in previous sections, the IEEE 802.15.4 standard defines PHY and MAC layers for low power and low data rate devices. Although the standard specified three different frequency bands, 2.4 GHz band has been mostly chosen due to its global availability. A total of 16 channels are available in this ISM band, each with a bandwidth of 2 MHz and a channel separation of 5 MHz. This band is not specified only for operation of WSNs and other wireless technologies like WLAN, bluetooth, and cordless phone are also operate in this band. One of the major competitors of WSNs in this band is WLAN based on IEEE 802.11. The IEEE 802.11 standard defines 22 MHz bandwidth for PHY in 2.4 GHz band that is much wider than operational bandwidth of IEEE 802.15.4. Specifically, each IEEE 802.11 channel overlaps with four consecutive channels of IEEE 802.15.4. Transmission power of IEEE 802.11 devices is another issue that is usually 15-20 dB higher than that of the IEEE 802.15.4. For these reasons, the operation of WSNs is highly influenced by operation of other collocated wireless devices in this licensed free band. Co-channel interference may easily corrupt packet transmissions of WSN nodes and leads to high packet drop in the network, which reduces the performance and reliability of the network. Nowadays, because of the widespread deployment of WLAN devices and introduction of IEEE 802.11n with 40 MHz operating bandwidth, it is less probable to find an interference-free channel for operation of IEEE 802.15.4 networks without disturbance from other wireless devices. In these hostile environments, it is wise to search for channels which provide more reliable link connectivity.

Ranking available channels is a helpful solution to ameliorate the performance of WSNs by determining channels for operation according to the merit of link performance. If all nodes in a network maintain channel ranks, they can come up with a common channel to operate on. Another use of channel ranking is in multi-channel communication protocol, in which each node can transmit data to another node on preferred channel. Channel ranking also improves the performance of networks utilizing adaptive frequency hopping schemes by providing list of reliable channels. In this thesis we try to rank channels based on achievable PDR on each channel. Since finding the PDR through packet transmissions consumes lots of energy, we present a method to estimate the achievable PDR on each channel by spectrum measurements.

Section 4.1 demonstrates system model of WSN which is considered in this thesis. Section 4.2 explains the metric used for channel ranking purpose. Section 4.3 explains the PDR and how it can be achieved in a direct way. Section 4.4 introduces the way to measure SINR for packet transmission in a channel. Section 4.5 explains the channel scanning scheme used to identify noise and interference characteristic on channels. Section 4.6 reviews the necessary mathematical equations which are needed for PDR estimation. In Section 4.7, PDR estimation methods for different channel conditions are presented.

4.1 System Model

The scenario we considered comprised of a link connection established by two low power wireless sensor nodes operate based on the IEEE 802.15.4 standard. These nodes operate over an unlicensed spectrum band partitioned into M orthogonal channels $\{c_1, c_2, ..., c_M\}$. A transmitter node S_{tx} can send data on one of the mentioned channels with a constant transmission power. Although transmission power of transmitter node is constant on all the channels, received signal power at receiver node S_{rx} may vary on each channel due to frequency selective fading. We use $\vec{S} = \{s_1, s_2, ..., s_M\}$ to denote the average received energy at the receiver node on each channel from the transmitter.

There may be other collocated wireless devices $(I_1, I_2, ...)$ operate in the same spectrum and induce interference to sensor link, we call these as interferer nodes. Unlike sensor nodes which operate on a single channel at a time, interferer nodes may use a subset of channels for their transmission according to PHY specifications. In addition, each interferer device has its own traffic pattern and transmission power. For the interferer I_i, we define channel occupancy as ρ_i and the interference strength P_i which indicates the perceived interference energy at the receiver node. Figure 17 illustrates the scenario which is considered in this thesis. A receiver node tries to estimate the achievable PDR on each channel by spectrum measurements and according to the received signal energy from transmitter node, i.e. $\vec{S}$. Afterwards, channels can be sorted according to the achieved PDR estimates.

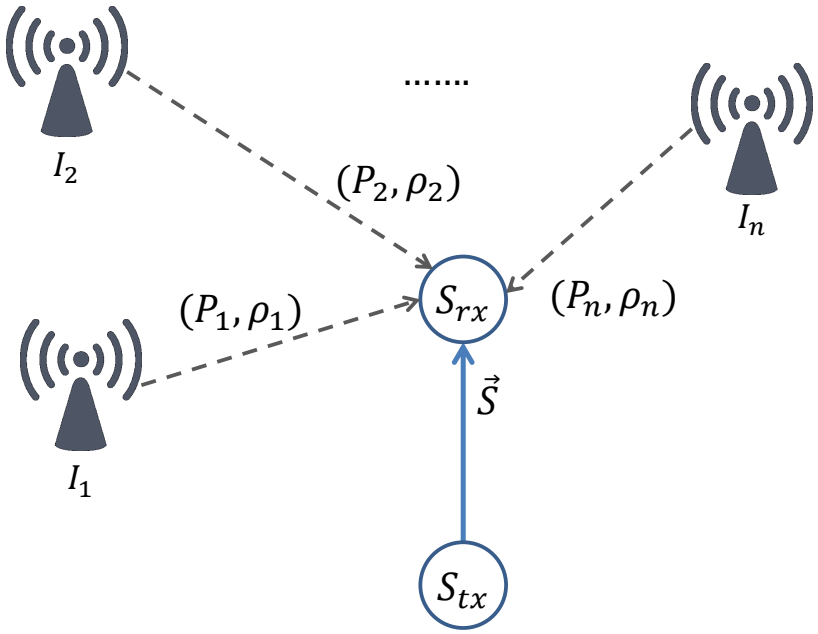

Figure 17: System model

4.2 Metric for Channel Ranking

In this thesis, the PDR is considered as a performance metric for channel ranking. The PDR is a common metric in WSNs to evaluate the performance of wireless link. The PDR can be defined as a function of SINR at the receiver node and traffic pattern of co-channel interferer in time domain. To rank channels for each link, receiver node requires estimating the achievable PDR on each channel by spectrum measurements. Obviously, knowing the noise and interference characteristics on a channel is not enough to predict the achievable PDR on a link, unless the received signal energy from transmitter pair of the link is known. Since received signal energy from the transmitter node can vary on channels due to frequency selective fading, some probe packet transmissions are required to find the received signal energy on each one. Afterwards, the receiver node is capable of estimating the PDR for each channel according to achieved information and arranging them in increasing order.

4.3 Packet Delivery Ratio

PDR is the ratio of the correctly received packets at the receiver to the total number of packets sent by the sender. A straightforward method to calculate PDR is to send a number of packets in a period of time. The receiver counts the successful received packets and calculates the PDR [43]. According to this definition, the PDR can be calculated as:

$$PDR = \frac{Number\ of\ received\ packets}{Number\ of\ transmitted\ packets}$$

High value for PDR indicates that wireless channel has a good condition, while low value for PDR presents that wireless channel is not in a proper condition and packet retransmissions are required to compensate packet drops. Consequently, power consumption and delay in system are increased and result in low network performance. Naturally, wireless link quality is subject to environment changes and prone to distortion, channel fading, noise and interference. These parameters make PDR to change dramatically over time. In order to obtain a reliable estimate of channel condition with achieved PDR criterion, packet transmissions should be performed with large number of packets, during a long period of time compared to coherence time of the channel. The coherence time is a statistical measure of the time duration over which the channel can be considered constant [44]. In other words, coherence time is the time duration in which any two received signals have a strong correlation. On the other hand, since sensor nodes are mostly powered by batteries and are expected to operate for a long period of time, calculating PDR with transmitting and receiving a large number of packets would consume too much energy. However, we use this empirical method in experiments as a reference to compare with PDR estimation results and explore how much the estimates are accurate.

4.4 Interference Measurement

The SINR defines the ratio between average received energy power from desired signal to power from interference and noise. The IEEE 802.15.4 PHY does not report this value directly and only provides RSSI value which indicates the strength of received signal. The definition of SINR and RSSI are given in (1) and (2) respectively.

$$SINR = 10log(\frac{S}{I+n}) \tag{1}$$

$$RSSI = 10log(S+I+n) \tag{2}$$

where S is the signal power, I is the interference power and n is the noise power. In this thesis the term SINR is abused as the difference between the average RSSI of the desired received packets and the average RSSI of the interference, hereafter stated as SINR*. According to this definition, the SINR* is given in (3).

$$\begin{array}{rcl} SINR^* & = & RSSI_{Packet} - RSSI_{Interference+noise} \\ SINR^* & = & 10log(\frac{S+I+n}{I+n}) \end{array} \tag{3}$$

The PHY of sensor node reports the RSSI value for each received packet. To find the interference and noise energy, node should collect RSSI samples from the channel when other pair node in a link is not transmitting on the channel. The reported value for each collected noise and interference RSSI sample is realized of one of following hypotheses [9]:

$$X[n] = \begin{cases} W[n] & H_0 \\ Y[n] + W[n] & H_1 \end{cases}$$

where H_0 is the hypothesis corresponding to there is no interference at time instant that sample is collected, and H_1 to existence of interference. $W[n]$ is a noise sample and $Y[n]$ is the interference energy sample. To distinguish that obtained RSSI sample is from the interference or noise, each RSSI value from channel is compared with a threshold. If RSSI sample is greater than the threshold, it is assumed that it has come from interference, otherwise from noise. In [45], the optimal threshold is obtained to be as:

$$T = \sigma_n^2[dBm] + 5[dBm]$$

where σ_n^2 is the noise level. Since in our experiments, the desired received signal energy normally is much higher than noise power (at least 15 dB), any interfering signal with energy below than the threshold (T) does not disturb IEEE 802.15.4 packet transmissions.

4.5 Channel Energy Measurement

In order to gather information about noise and interference characteristics, sensor node scans each channel separately. Section 4.5.1 presents the channel sensing scheme. Some modifications are required for OS to implement this sensing method on the sensor platform. Section 4.5.2 describes these modifications.

4.5.1 Channel scanning scheme

This section presents the channel scanning scheme which is used to gather information about noise and interference on the channel. The PDR estimation algorithm utilizes these information to predict the achievable PDR on each channel for a given signal strength from the transmitter node. In channel scanning procedure, the receiver node requires collecting samples from noise and interference on the channel, hence during this procedure, the IEEE 802.15.4 transmitter node should prevent transmitting data on the channel which is being scanned. Once scanning of one channel is finished, the receiver node switches to another candidate channel and repeats the scanning procedure. This process continues until all channels have been scanned. Hereafter, we focus on a single receiver node which intends to scan channel c_i. Node collects L macro-samples from the channel periodically. Time spacing between two consecutive macro-samples are constant and equal to T_I. Each macro-sample consist of k micro-samples. These k micro-samples are uniformly distributed over a period time of T_S. This channel scanning strategy is depicted in Figure 18.

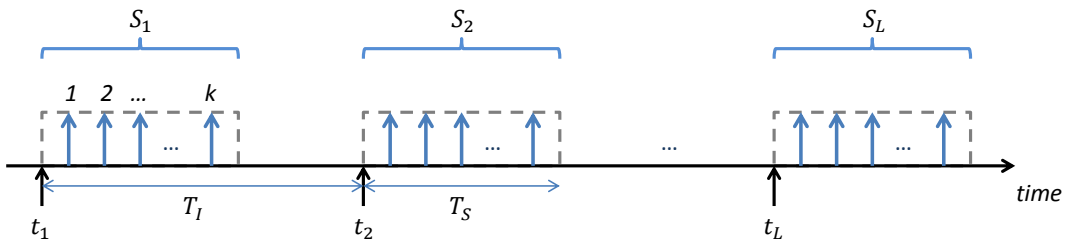

Figure 18: Sketch of the channel scanning algorithm

4.5.2 Channel scanning implementation

In a channel scanning procedure, it is required to collect samples from the channel. These samples can be obtained through reading the RSSI from the radio chip. In conformance with the IEEE 802.15.4 standard the CC2420 provides the current RSSI by software [46]. When the radio is in an active mode, it continuously updates and averages the RSSI over the last 8 symbol periods, i.e. 128 μs. The FreeRTOS allows to read this value through a function called $rf\_analyze\_rssi$. By calling this

function, it turns on the radio chip and waits until the RSSI register becomes valid. Then the function reads the RSSI register eight times every 16 μs. Finally, it turns off the radio and reports the average of eight RSSI samples as an 8-bit integer value. Sampling frequency using this defined function is less than 5 kHz. Averaging the eight RSSI samples leads that the reported value is averaged over 16 symbol periods, i.e. 256 μs.

In order to improve the PDR estimation based on channel scanning, it is essential to collect samples from the channel with higher frequency. To achieve this goal, a new function is provided called as $rf\_analyze\_rssi\_HF$. This function receives two parameters, the first defines how many samples should be collected from the channel, and the second defines the address that collected samples should be stored. This function first turns on the radio chip and waits until the RSSI register becomes valid. Then it collects samples every 16 μs and stores each one separately. When all the specified samples are collected, the function turns off the radio and returns. Using this function leads that the channel is scanned and RSSI values are collected with frequency of 62.5 kHz. The implementation of sampling RSSI from channel with high frequency can be found in the Appendix D.

4.6 Mathematical Model

The PHY of the IEEE 802.15.4 at 2.4 GHz frequency employs O-QPSK with half-sine pulse shaping for modulation which is equivalent to Minimum Shift Keying (MSK). In Additive White Gaussian Noise (AWGN) channel, signal strength is constant at the receiver and only noise may lead that the receiver detects a bit erroneously. If E_b/N_0 is the ratio between the average energy of bit and the noise power spectral density at the IEEE 802.15.4 receiver node, the bit error rate of O-QPSK can be expressed as:

$$P_b = Q(\sqrt{\frac{2\gamma E_b}{N_0}}) \tag{4}$$

where:

$$Q(x) = \frac{1}{\sqrt{2\pi}} \int_{\infty}^{x} exp(-\frac{u^2}{2}) du \tag{5}$$

and $\gamma \approx 0.85$ [47]. In the presence of interference in the environment, E_b/N_0 should be replaced by $SINR$ in (4), where $SINR$ is the ratio between received energy of the bit to the energy of the noise and interference at receiver input at time instant of receiving the bit. The bit error probability function can be revised as:

$$P_b(SINR) = Q(\sqrt{2\gamma SINR}) \tag{6}$$

A receiver node can detect a packet without error if all its bits are received correctly. For a packet consists of N bits, the probability of receiving the packet correctly is product of probabilities of receiving all individual bits:

$$P_{no\,error} = \prod_{i=1}^{N}(1 - Q(\sqrt{2\gamma SINR_i})) \tag{7}$$

where $SINR_i$ is the $SINR$ corresponding to the ith bit.

4.7 PDR Estimation

This section presents how it is possible for a node to predict the achievable PDR of a sensor link by using channel sensing algorithm. The receiver node should adapt the channel scanning scheme to traffic from its communication pair. To achieve this goal, following assumptions have been made:

- The IEEE 802.15.4 transmitter node intends to send packets periodically with rate of P packets/sec. Each packet consists of N bits and data rate of IEEE 802.15.4 is equal to R bits/s. This is a typical traffic model for sensor networks where a node needs to regularly report data to the sink.

- To estimate the achievable PDR, the receiver node collects samples from channel as described in Section 4.5.1. L macro-samples are collected periodically with the same rate that transmitter node intends to transmit packets ($T_I = 1/P$). Each macro-sample consists of k micro-samples, and the number of micro-samples in each macro-sample is less than the number of bits within a packet ($k < N$). In addition, micro-samples are uniformly collected over the period equal to IEEE 802.15.4 packet transmission time ($T_S = N/R$).

- Coherence time of the channel for sensor link is greater than a packet transmission time of IEEE 802.15.4; hence the received signal energy for a packet transmission remains constant for all its bits.

- Interference and channel condition varies slowly compared to the sampling frequency of micro-samples. In this way, noise and interference remain almost constant for duration of T_S/k.

Section 4.7.1 presents the PDR estimation method for a channel conditions that IEEE 802.15.4 nodes have a constant link and received signal energy from transmitter node remains constant for all the packet transmissions. Section 4.7.2 and Section 4.7.3 suggest two methods for PDR estimation in the channel conditions that received signal energy from transmitter node may vary over time.

4.7.1 PDR estimation for a constant link connection

When signal from IEEE 802.15.4 transmitter does not fade in the channel, received signal strength can almost be assumed to be constant for all packet transmissions at receiver node. This assumption generally does not hold for wireless channels, since channel may vary over the period of use. However, for a link connection with a strong LOS path, received signal can be considered approximately constant. Hence all the packets and their bits are received with the same signal energy. In such condition, SINR for each bit within a packet only depends on changing the noise and interference level.

First, it is desired to find the probability that receiver node could have received a packet if transmitter node had sent a packet at time instant that jth macro-sample was collected. Since it is assumed that noise and interference alter slowly compared to the time between two consecutive micro-samples within a macro-sample, each micro-sample can present the noise and interference level that N/k bits could have experienced. The probability of reception of packet is derived from (7) and is given in (8).

$$P_{no\,error} = \prod_{i=1}^{k} (1 - Q(\sqrt{2\gamma SINR^*_{j,i}}))^{(\frac{N}{k})} \tag{8}$$

where $SINR^*_{j,i}$ corresponds to the difference between received signal energy of bit and ith micro-sample in jth macro-sample. According to this definition $SINR^*_{j,i}$ is given in (9).

$$SINR^*_{j,i} = RSSI_{Packet} - (RSSI_{Interference+noise})_{j,i} \tag{9}$$

The PDR estimate can be calculated by averaging the probabilities of receiving packets correctly according to all L collected macro-samples. The PDR estimate is given in (10).

$$PDR_{estimate} = \frac{1}{L} \sum_{j=1}^{L} \prod_{i=1}^{k} (1 - Q(\sqrt{2\gamma SINR^*_{j,i}}))^{(\frac{N}{k})} \tag{10}$$

4.7.2 PDR estimation for varying channel based on average signal strength

In real environments, desired received signal strength from transmitter node may vary over time at the receiver node due to fading in the channel. In this case SINR for each bit may vary because of the change in received signal strength or change in noise and interference level. One way to simplify this situation is to use the average energy for all packet transmissions. To calculate the average received energy in a channel, transmitter node should send some packets and receiver node store the RSSI values of received packets. If M packets are received by receiver node, average

signal energy can be obtained as:

$$\overline{RSSI_{Packet}} = \frac{1}{M}\sum_{q=1}^{M}(RSSI_{Packet})_q \tag{11}$$

where $(RSSI_{Packet})_q$ corresponds to the RSSI value of qth received packet. According to the definition of average signal strength, we can define $\overline{SINR^*_{j,i}}$ which is the difference between the average energy of received packets and the RSSI value of ith micro-sample of jth macro-sample. According to this definition $\overline{SINR^*_{j,i}}$ is given in (12).

$$\overline{SINR^*_{j,i}} = \overline{RSSI_{Packet}} - (RSSI_{Interference+noise})_{j,i} \tag{12}$$

Now, we can find the probability that receiver node could have received a packet correctly, if a transmitter node had transmitted a packet when jth macro-sample was collected. The probability is derived from (8) and is given in (13), assuming that the average received energy for packet transmissions is known.

$$P_{no\,error} = \prod_{i=1}^{k}(1 - Q(\sqrt{2\gamma\overline{SINR^*_{j,i}}}))^{(\frac{N}{k})} \tag{13}$$

The PDR estimate can be calculated by averaging the probabilities of receiving packets correctly according to the all L collected macro-samples:

$$PDR_{estimate} = \frac{1}{L}\sum_{j=1}^{L}\prod_{i=1}^{k}(1 - Q(\sqrt{2\gamma\overline{SINR^*_{j,i}}}))^{(\frac{N}{k})} \tag{14}$$

In this method we take into account the effects of fading on IEEE 802.15.4 signal by using average received signal strength over all received packets.

4.7.3 PDR estimation for varying channel based on signal strength distribution

As noted in previous section, signal strength of received packets may vary because of the fading over time. Another method to take into account the effect of fading on IEEE 802.15.4 link is to use energy distribution of received packets in our PDR estimation. Since it is considered that channel condition changes slowly compared to the IEEE 802.15.4 packet transmission time (coherence time of the channel is greater than the packet transmission time of IEEE 802.15.4), received signal energy for all the bits in a packet can be assumed to be constant, while signal energy can vary from packet to packet.

To obtain information about the received signal energy distribution, transmitter node should send some packets and receiver node store the RSSI values from received packets. These set of received signal strength from packets can present the distribution of received energy on the channel if packets are transmitted over a long period of time compared to the coherence time of the channel, and the number of

transmitted packets are large enough. Hence it is expected that received energy of other packet transmissions at other times have the same distribution. We assume that IEEE 802.15.4 receiver node received M packets from transmitter, and L macro-samples was collected with k micro-samples for each. we can define $SINR_{q,j,i}$ as the difference between RSSI value of qth received packet and ith micro-sample in jth macro-sample. According to this definition, $SINR_{q,j,i}$ is given in (15).

$$SINR_{q,j,i} = (RSSI_{Packet})_q - (RSSI_{Interference+noise})_{j,i} \tag{15}$$

The probability that receiver node could have received a packet correctly if received power had been equal to the signal strength of qth received packet, and packet had been transmitted during time which jth macro-sample was collected can be presented as:

$$P_{no\,error} = \prod_{i=1}^{k} (1 - Q(\sqrt{2\gamma SINR^*_{q,j,i}}))^{(\frac{N}{k})} \tag{16}$$

If fading for IEEE 802.15.4 and IEEE 802.11 links are independent from each other, it can be assumed that received signal strength from IEEE 802.15.4 for later packet transmissions in the channel will have one of the signal levels of M packets that have been received. If we assume that for each packet transmission effect of interference and noise can be like with one of L macro-samples that were collected, PDR estimate can be calculated by considering all the combination of M received signal strength levels and all L macro-samples. The PDR estimate according to this method is given in (17).

$$PDR_{estimate} = \frac{1}{L \cdot M} \sum_{q=1}^{M} \sum_{j=1}^{L} \prod_{i=1}^{k} (1 - Q(\sqrt{2\gamma (SINR^*_{q,j,i})}))^{(\frac{N}{k})} \tag{17}$$

5 PDR Estimation Performance

Different measurements are carried out under various circumstances to evaluate the performance of the proposed PDR estimation method under variety of interference patterns and channel models. In Section 5.1, the observations and results for Gaussian channel is presented. Section 5.2 presents the observations and results for experiments in which only interferer link faces fading, while Section 5.3 presents observations and results that both the IEEE 802.15.4 and IEEE 802.11 interferer signals fades in the channel. The effectiveness of PDR estimation based approach for ranking the channels are investigated by applying the proposed method to rank the IEEE 802.15.4 channels in a real environment. The detailed results are presented in Section 5.4. Finally, the development and application of the channel ranking in a large network is discussed in Section 5.5.

5.1 Gaussian Channel

This experiment is performed according to the setup introduced in Section 3.1.1. IEEE 802.15.4 and IEEE 802.11 links do not experience any fading. In wired connection, since there is no fading in the channel, received signal from transmitter node remains almost constant. Noise characteristic for this setup can be modeled as AWGN with a constant spectral density and a Gaussian distribution of amplitude.

As mentioned in Section 3.5, we consider a scenario that IEEE 802.15.4 transmitter node intends to send fixed-size packets periodically every 30 ms. Packet size is 62 bytes and packet transmission time for each packet is 1984 μs. We want to evaluate the capability of IEEE 802.15.4 receiver node to predict the achievable PDR by spectrum measurements under different interference conditions. To achieve this goal, the receiver node scans the channel and collects 50 macro-samples every 30 ms according to the methodology described in Section 4.5.1. Each macro-sample consists of 125 micro-samples which are collected during 1984 μs (macro-samples are collected every 16 μs). This duration is equal to transmission time of a IEEE 802.15.4 packet with 62 bytes size. Collected samples are sent to the computer to estimate the PDR for different signal strength levels. Section 5.1.1 presents the analysis of collected samples from the channel. To evaluate the accuracy of PDR estimation, the PDR is also calculated in the direct way through packet transmissions in the channel as introduced in Section 4.3. These results are presented in Section 5.1.2.

5.1.1 Channel scanning results

In order to provide different interference patterns, different periodic traffics are generated by use of MGEN traffic generator, using different packet rates and payload sizes. In the first experiment, payload size of IEEE 802.11 is kept constant at 500 bytes for each packet. Four different traffic patterns are generated by using packet rates of 100, 300, 500 and 700 packets/s. The IEEE 802.15.4 receiver node collects

samples from each traffic pattern. Results of the first ten macro-samples for these four traffic patterns are presented in Figure 19.

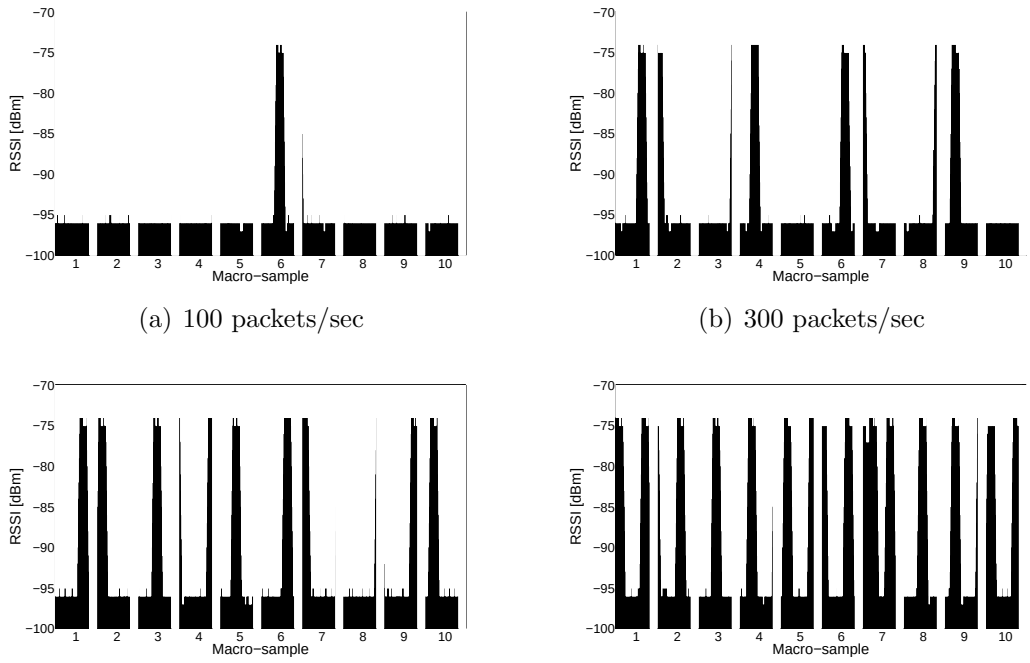

(a) 100 packets/sec

(b) 300 packets/sec

(c) 500 packets/sec

(d) 700 packets/sec

Figure 19: Captured macro-samples for variable number of packets/sec of IEEE 802.11 (with 500 bytes payload size), RSSI vs. macro-sample (each macro-sample is captured during 1984 μs)

Observation 1 (Figure 19): The low RSSI values show the energy of noise floor which is around -97 dB. There are also small fluctuations around the noise level that prove noise floor is not completely constant.

Observation 2 (Figure 19): In some of macro-samples, there are big spikes which show that IEEE 802.11 transmitted packets at that time instances. The maximum level of these spikes is around -74 dB which indicates the maximum perceived interference level from IEEE 802.11 at the receiver node in this particular experiment.

Observation 3 (Figure 19): Some of the IEEE 802.11 packet transmissions are happened completely during macro-sample windows while some others partially overlapped with first or last parts of macro-sample windows. The duration of IEEE 802.11 packet transmissions happened completely within a macro-sample window, are constant since the packet payload size is kept fixed.

Observation 4 (Figure 19): Level of some spikes that partially overlapped with macro-sample windows (Like 7th macro-sample in Figure 19(a)) are not as high as

energy of packet transmissions that are happened completely during macro-sample windows. This is because of averaging of the RSSI value over 8 symbols and these samples show the average energy of interference and noise floor. In fact even for packets that are completely captured with sampling windows, the first and last 7 collected samples from interference are below the maximum received level, where are not visible because of the high density of the collected samples. To illustrate this fact, Figure 20 shows the 6th macro-sample of Figure 19(a) in enlarged scale.

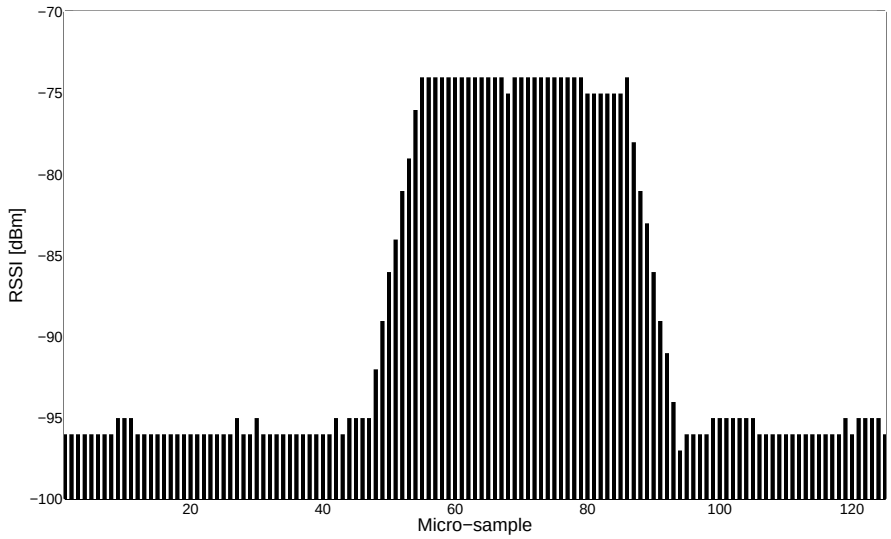

Figure 20: Captured micro-samples from IEEE 802.11 (100 packets/sec, 500 bytes payload size)

Observation 5 (Figure 19): By increasing the packet rate of IEEE 802.11 interferer, more macro-samples are collided with packet transmissions from interference. This increment continues until all the macro-samples are collided at least with one packet transmission from IEEE 802.11. It can be observed that all macro-samples are collided for packet rates more than 500 packets/sec from interferer.

Observation 6 (Figure 19): Higher packet rate of IEEE 802.11 leads to the fact that packets are transmitted more frequently and it is possible for very high number of packet/s that more than one packet transmissions are happened within a macro-sample window. In Figure 19(d) when packet rate is 700 packets/sec, eight of macro-samples are collided with two packet transmissions (macro-samples 1, 2, 4, 5, 6, 7, 9 and 10).

For the second experiment, number of packets/sec from IEEE 802.11 is kept fixed while payload size of packets is changed. Four different traffic patterns are generated by using payload sizes of 100, 300, 500 and 700 bytes. The IEEE 802.15.4 receiver node collects samples from each traffic pattern. The first ten collected

macro-samples from each traffic pattern are shown in Figure 21.

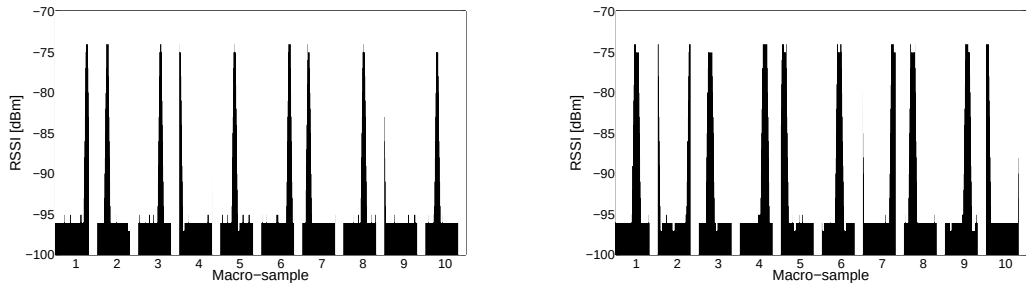

(a) 100 bytes payload size

(b) 300 bytes payload size

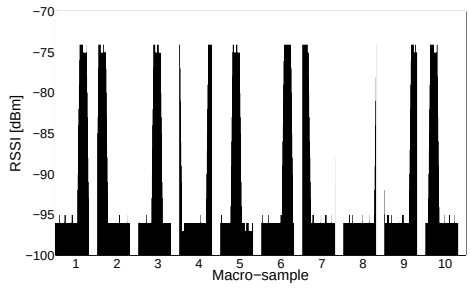

(c) 500 bytes payload size

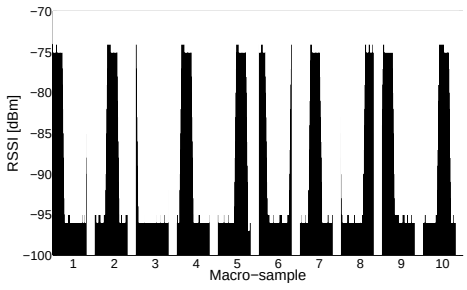

(d) 700 bytes payload size

Figure 21: Captured macro-samples for variable payload size of IEEE 802.11 (with 500 packets/sec), RSSI vs. macro-sample (each macro-sample is captured during 1984 μs)

Observation 7 (Figure 21): Without considering the payload sizes, it can be observed that all of macro-samples are collided with 500 packets/sec data transmissions from IEEE 802.11.

Observation 8 (Figure 21): Higher payload size in packet transmissions leads to increase in collision time during macro-sample windows.

According to these two experiments we can conclude that:

Observation 9 (Figure 19 and Figure 21): Number of collided macro-samples is highly affected by the number of packets/sec and is independent from the payload size of packets.

Observation 10 (Figure 19 and Figure 21): Collision time of the collided macro-samples mostly depends on the payload size of packets from interferer. In fact more payload size causes higher collision time for collided macro-samples. In addition, the collision time of collided macro-samples is also increased for interference with very high number of packets/sec, where more than one packet transmission happen

during one macro-sample.

5.1.2 PDR estimation results

This section evaluates the accuracy of PDR estimation based on channel scanning by comparing with the empirical PDR results achieved by packet transmissions through the channel. The empirical PDR is measured by packet transmissions according the methodology described in Section 3.5 for each traffic condition from interferer and signal strength level from transmitter node. The IEEE 802.15.4 transmitter node sends 1000 packets periodically, every 30 ms through the channel. The receiver node stores the RSSI values for received successful packets. It also collects a RSSI sample from the channel just after reception of each packet and compares it with threshold to distinguish if it is noise power or interference power. When the packet transmission is finished, the IEEE 802.15.4 receiver node calculates the average SINR* by finding the difference between average RSSI from received packets and average of RSSI samples from interference. Finally, calculated PDR and average SINR* are reported to the computer. The signal strength of IEEE 802.15.4 transmitter node is changed with the aid of an attenuator and packet transmissions are repeated to achieve the PDR ranging from 0 to 100%. This procedure also repeated for different interference traffics to ensure that PDR estimation method is reliable regardless of the traffic pattern.

The PDR estimate for each traffic pattern from the interferer is obtained from 50 collected macro-samples. Each macro-sample is collected during 1984 μs and consist of 16 micro-samples. Micro-samples are collected every 128 μs during each macro-sample, and each micro-sample reports the average energy during 128 μs. Hence these 16 samples completely cover the scanning window ($16 \times 128\mu s \approx 1984\mu s$). The PDR is estimated for different signal strength levels based on (10). However, it is observed that the value $\gamma = 1.75$ provides the most accurate estimates. This values is used for all other estimates in the rest of this thesis. The main reason for this difference is the unavoidable inaccuracy in the RSSI samples, since reported RSSI values has $\pm$ 6 dB variation. To plot the estimated PDR along with empirical PDR obtained from packet transmissions, they are also plotted as a function of SINR*. Interference level is calculated according to collected samples from the channel. Average interference level is calculated by averaging the RSSI samples that are greater than the threshold.

The first PDR estimates belong to the first experiment introduced in Section 5.1.1 in which the payload size of packets form interferer is kept fixed. Four different periodic traffic patterns are generated by using packet rates of 100, 300, 500 and 700 packets/sec. Figure 22 present the PDR estimates and empirical PDR results obtained through packet transmissions for each traffic pattern from the interferer.

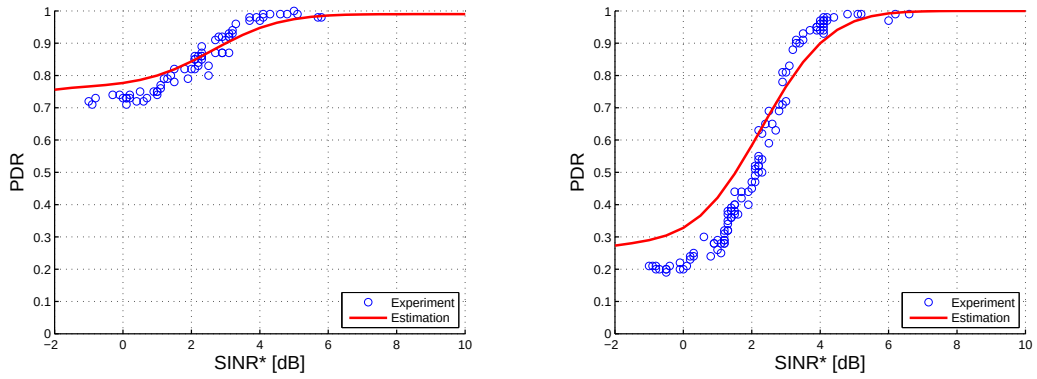

(a) 100 packets/sec

(b) 300 packets/sec

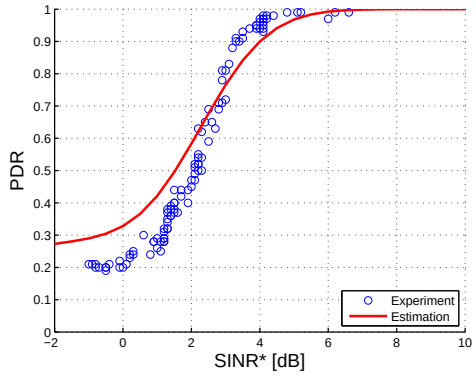

(c) 500 packets/sec

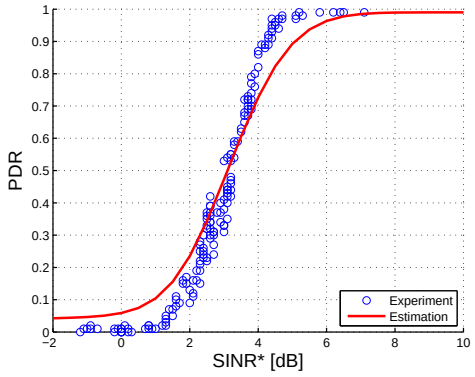

(d) 700 packets/sec

Figure 22: Estimated and empirical PDR for variable number of packets/sec of IEEE 802.11 (with 500 bytes payload size), PDR vs. SINR* , (Gaussian channel for IEEE 802.15.4 and IEEE 802.11 links)

Following observations can be obtained according to Figure 22:

Observation 11 (Figure 22): The PDR estimates follow very closely the empirical results with less than 10% error.

Observation 12 (Figure 22): When the SINR* is greater than 6 dB, almost all of the packets are received correctly by IEEE 802.15.4 receiver node regardless to the traffic pattern from IEEE 802.11. This region where all packets can be received correctly is called perfect packet reception region [48].

Observation 13 (Figure 22): In the case of the SINR* being less than 0 dB, the PDR in each condition remains almost constant. Since the SINR* is very low in this region, only packets that are not collided with packet transmissions from IEEE 802.11 can be received correctly. As a result, the PDR is independent of SINR* in this region.

Observation 14 (Figure 22): When the number of packets/sec from IEEE 802.11 is more than 500 packets/sec and the SINR* is low, all packets are corrupted with interferer and there is no chance to receive a packet correctly. The region where the PDR is zero is called zero packet reception region. This region exists only when interference traffic from IEEE 802.11 is more than 500 packets/sec. This fact is pursuant to the results presented in Figure 19 in which all the macro-samples are collided with packet transmission rates more than 500 packets/sec.

5.2 Fading Channels for IEEE 802.11 Interferer

The purpose of this experiment is to assess the accuracy of PDR estimation in conditions that interferer link experiences fading in the channel. The setup introduced in Section 3.1.1 is used for this purpose in which IEEE 802.15.4 signal experiences the Gaussian channel, while IEEE 802.11 interferer signal undergoes fading channel. The measurement is carried by emulating three different channel models described in Section 3.4.3. Mobile speed in channel emulator is set as 3.6 km/h which is comparable with the speed of movements in indoor environments.

Like previous section, the IEEE 802.15.4 transmitter node intends to send fixed-size packets periodically every 30 ms. Packet size is 62 bytes and packet transmission time for each packet is 1984 μs. The receiver node tries to predict the achievable PDR for each interferer condition by spectrum measurements. It scans the channel and collects 50 macro-samples every 30 ms as described in Section 4.5.1. Each macro-sample consists of 16 micro-samples and are collected during 1984 μs. Section 5.2.1 presents the analysis of collected samples from the channel. The PDR estimation results are compared with empirical PDR obtained through packet transmissions and are presented in Section 5.2.2. Effect of number of collected samples on accuracy of PDR estimation is investigated in Section 5.2.3.

5.2.1 Channel scanning results

In order to realize the effect of environmental variations on the interferer link, a common traffic pattern is used for different channel models. A periodic traffic is generated with fixed 500 packets/s and 500 byte payload size as a source of interference, while three different channel models introduce in Section 3.4.3 are simulated for IEEE 802.11 link. Receiver node collects 30 macro-samples from the faded interferer signal in each channel model and results are shown in Figure 23.

Observation 15 (Figure 23): Since channel varies very slowly, it can be observed that received signal strength for each packet transmission remains almost constant during each macro-sample (signal energy from interferer does not fluctuate over each macro-sample, but it changes over different macro-samples). Hence the channel can be assumed that not change during a macro-sample duration and the coherence time

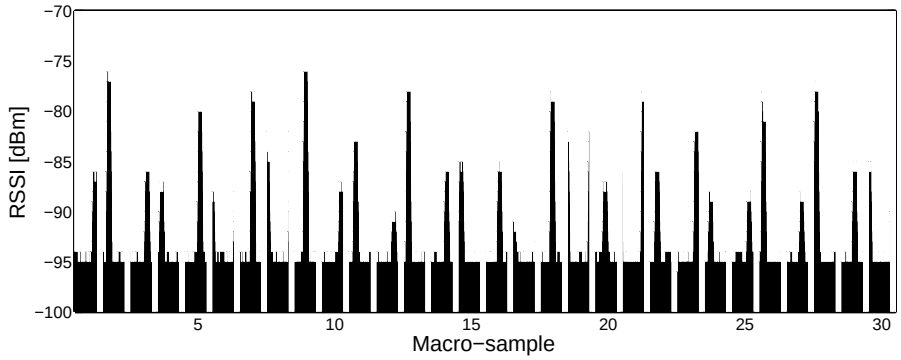

(a) Channel model A

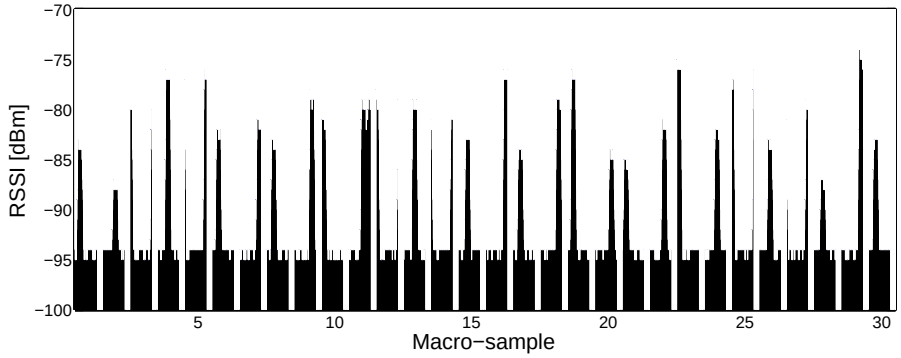

(b) Channel model D

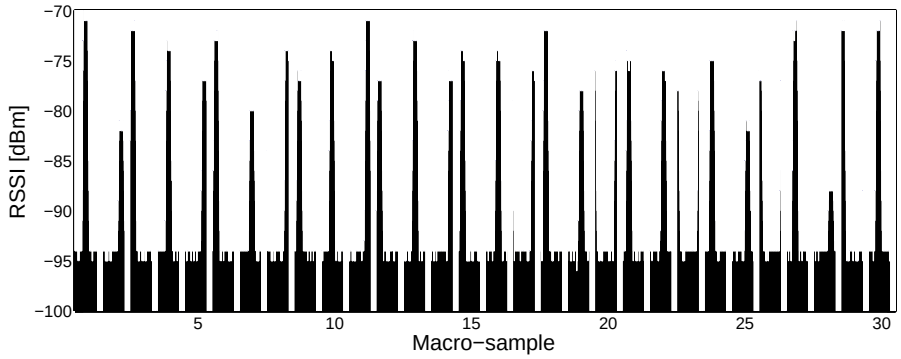

(c) Channel model TGn B

Figure 23: Captured macro-samples for a fixed traffic pattern from IEEE 802.11 (500 packets/sec, 500 bytes payload size) in different fading channels, RSSI vs. macro-sample (each macro-sample is captured during 1984 μs)

of the channel is greater than IEEE 802.15.4 packet transmission time.

Observation 16 (Figure 23): In channel model A which models a NLOS condition, the variation of received signal over macro-samples are more compared to channel model D and channel model TGn B which model LOS conditions.

Observation 17 (Figure 23): The average received energy from IEEE 802.11 interferer in channel model TGn B which models wireless channel for small environments is higher than other channel models.

5.2.2 Estimation results

Detailed measurements are carried out to understand the accuracy of PDR estimation method under various interferer traffic patterns and in various fading channel models for interferer link. For each channel model, different traffics are generated by varying the number of packets/sec while payload size of packets is kept fixed as 500 bytes. Four different traffic patterns are generated by using packet rates of 100, 300, 500 and 700 packets/s.

In the first experiment, channel model TGn B that models small environment wireless channels is applied for interferer link. IEEE 802.15.4 nodes are connected through the wired connection and experience the Gaussian channel. PDR estimation results are obtained from spectrum measurements, while empirical PDR is obtained through packet transmission through the channel. Estimated PDR and empirical results for this channel model are plotted in Figure 24.

Observation 18 (Figure 24): The PDR estimates follow the experimental PDR results closely with less than 15% error.

Observation 19 (Figure 24): If the SINR* is greater than 13 dB, the receiver node is capable of receiving all the packets correctly regardless of the interference activity of IEEE 802.11.

Observation 20 (Figure 24): In case SINR* is less than -9dB and the packet rate of IEEE 802.11 interferer is higher than 500 packets/sec, all transmitted packets by IEEE 802.15.4 are collided and there is no chance for the correct reception of IEEE 802.15.4 packets. Accordingly, zero packet reception region exists only when the packet rate from interferer is more than 500 packets/sec.

Second experiment is carried out by introducing the channel model A for NLOS condition for IEEE 802.11 link. The receiver node scans the channel and tries to predict the achievable PDR for different signal strength levels from the transmitter node. The PDR estimates and empirical PDR results obtained through packet transmissions are presented in Figure 25.

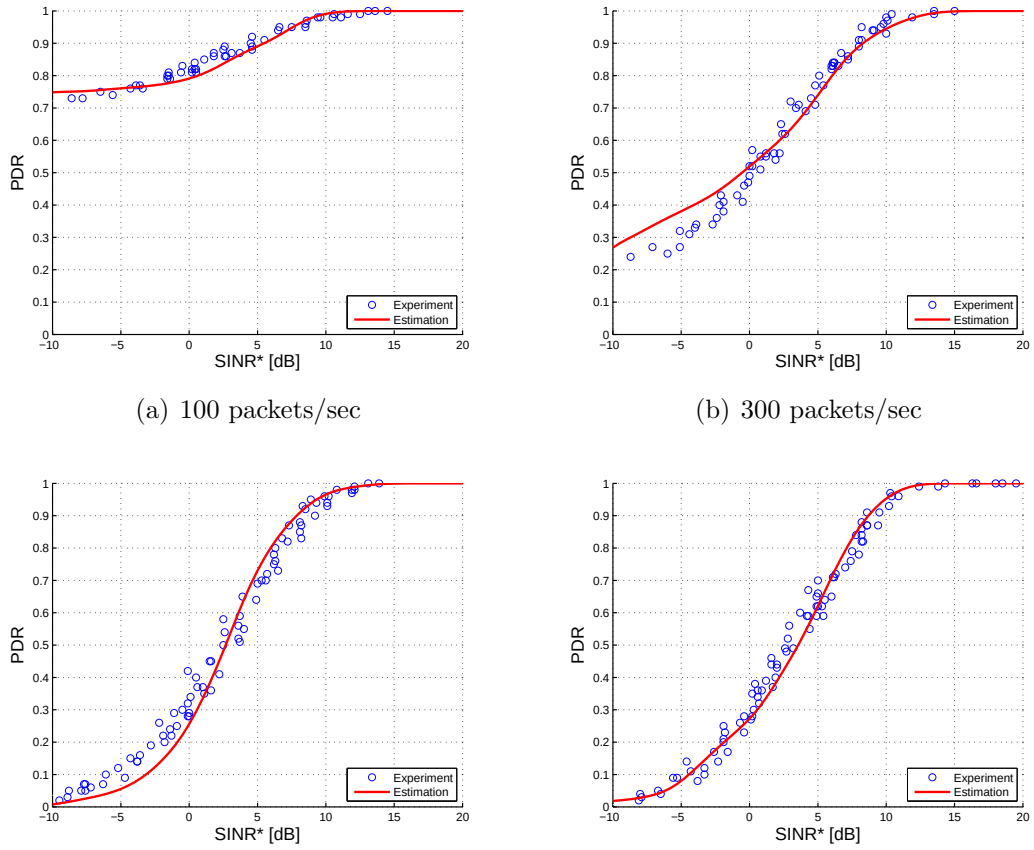

(a) 100 packets/sec

(b) 300 packets/sec

(c) 500 packets/sec

(d) 700 packets/sec

Figure 24: Estimated and empirical PDR results for variable number of packets/sec of IEEE 802.11 (with 500 bytes payload), PDR vs. SINR*, (Gaussian channel for IEEE 802.15.4 link, channel model TGn B for IEEE 802.11 link)

Observation 21 (Figure 25): It can be seen that differences between the estimated PDR and empirical are less than 10%.

Observation 22 (Figure 25): In this channel condition, all IEEE 802.15.4 packets can be received correctly irrespective to the interference activity of IEEE 802.11 when the SINR* is greater than 10 dB.

Observation 23 (Figure 25): It is noticeable that when the SINR* is less than -5 dB, the achieved PDR for each interferer traffic remains nearly constant.

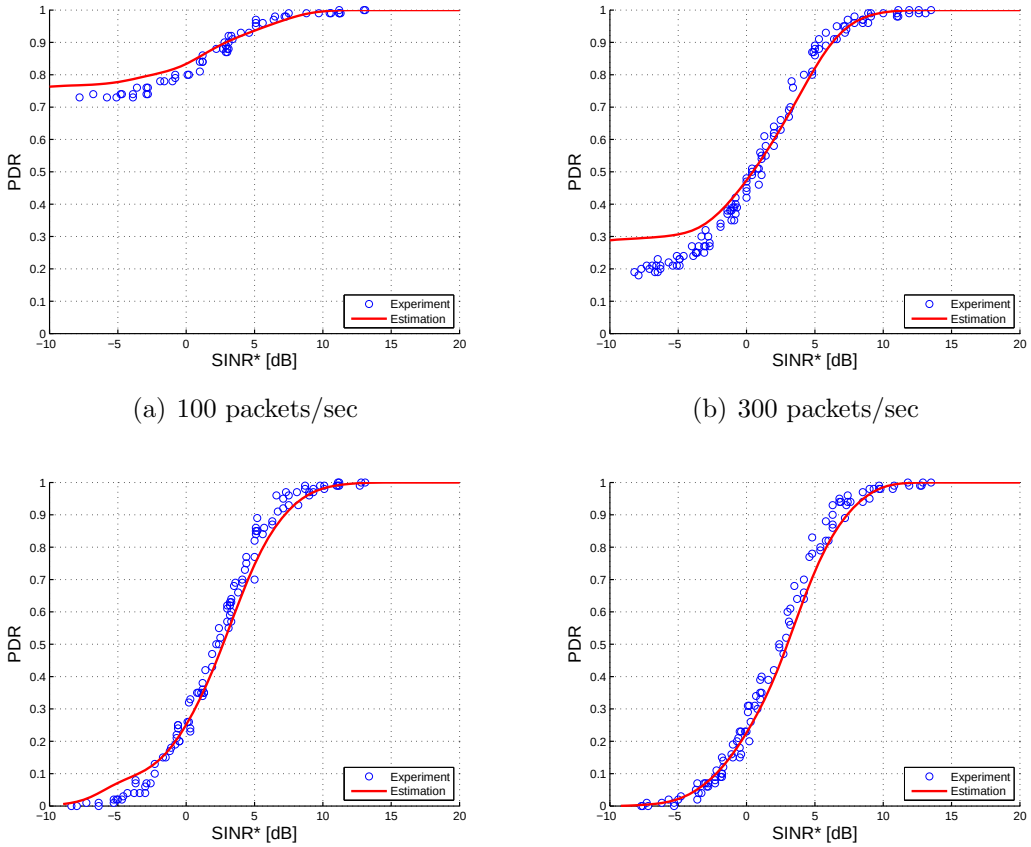

(a) 100 packets/sec

(b) 300 packets/sec

(c) 500 packets/sec

(d) 700 packets/sec

Figure 25: Estimated and empirical PDR results for variable number of packets/sec from IEEE 802.11 (with 500 bytes payload size), PDR vs. SINR*, (Gaussian channel for IEEE 802.15.4 link and channel model A for IEEE 802.11 link)

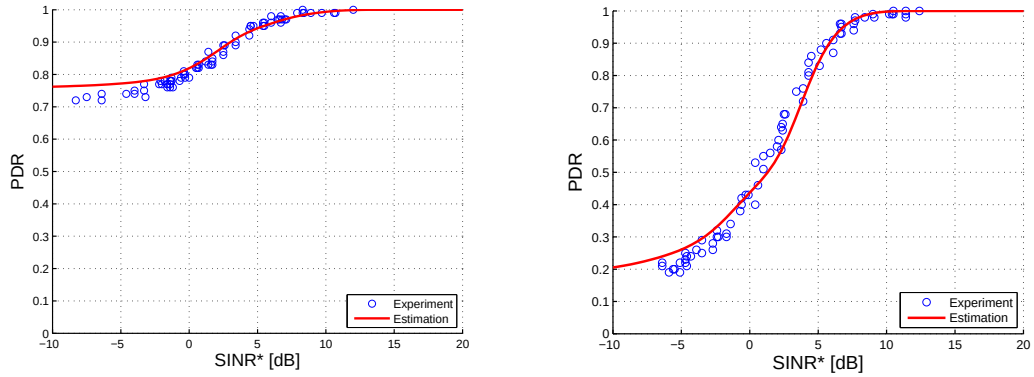

(a) 100 packets/sec

(b) 300 packets/sec

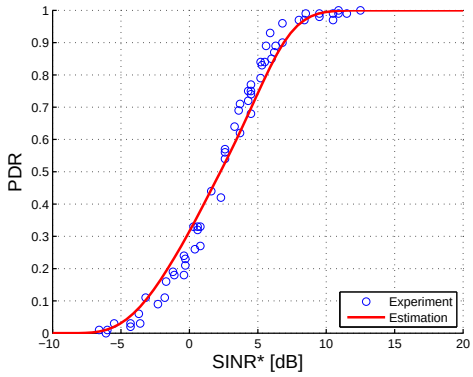

(c) 500 packets/sec

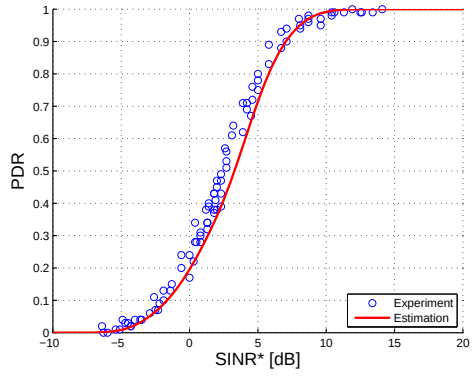

(d) 700 packets/sec

Figure 26: Estimated and empirical PDR results for variable number of packets/sec of IEEE 802.11 (with 500 bytes payload size), PDR vs. SINR*, (Gaussian channel for IEEE 802.15.4 link and channel model D for IEEE 802.11 link)

Lastly, channel model D for LOS condition is introduced to the IEEE 802.11 link to model a fading channel for interferer link. Measurements are repeated under different traffic patterns from the interferer. PDR estimates and empirical results are shown in Figure 26.

Observation 24 (Figure 26): The PDR estimation results follow the empirical PDR with less than 15% error in all traffic conditions.

Observation 25 (Figure 26): The SINR* for this setup should be greater than 12 dB in order that all packets from IEEE 802.15.4 transmitter are received correctly regardless of traffic pattern from IEEE 802.11 interferer.

Observation 26 (Figure 26): The PDR remains almost constant for each traffic pattern from IEEE 802.11 interferer when the SINR* is less than -5 dB.

5.2.3 Effects of number of samples on PDR estimation

The PDR estimation accuracy is highly dependent on number of collected samples from the channel; that is it depends on number of macro-samples (L), as well as number of micro-samples (k). Increasing the number of L and k improves the accuracy of the PDR estimation with cost of more energy consumption during channel scanning procedure. It is beneficial to perform the PDR estimation with the minimum number of samples providing the required accuracy. The purpose of this experiment is to determine the effect of collected samples from the channel on performance of the PDR estimation method.

In order to achieve this goal, setup depicted in Section 3.1.2 is used that only signal from IEEE 802.11 interferer fades in the channel. Channel model A introduced in Section 3.4.3 is configured for channel emulator which models a NLOS condition. This channel model is chosen since interferer signal fades more compared to other channel models that model a LOS condition. A periodic traffic is generated with fixed packet rate of 500 packets/s and 500 bytes payload size. To observe the effect of number of L and k separately, only one parameter is changed in each experiment while the other is kept fixed. In the first experiment, the number of macro-samples are changed whilst for each one 16 micro-samples are collected. This number of micro-samples is enough to completely cover the macro-sample scanning window. Three estimates are obtained by using 10, 20 and 30 macro-samples. The empirical PDR is obtained for different signal strength levels from the transmitter node through packet transmissions as used in previous measurements. Figure 27 presents PDR estimates obtained from different number of macro-samples and empirical PDR together.

Observation 27 (Figure 27): It can be observed that estimates obtained from 20 and 30 macro-samples follow the empirical PDR results precisely with less than 10% error, but the error for estimates with 10 macro-samples is greatar than this.

Observation 28 (Figure 27): For lower number of macro-samples, the PDR estimate is reliable on condition that the SINR* is greater than 4 dB.

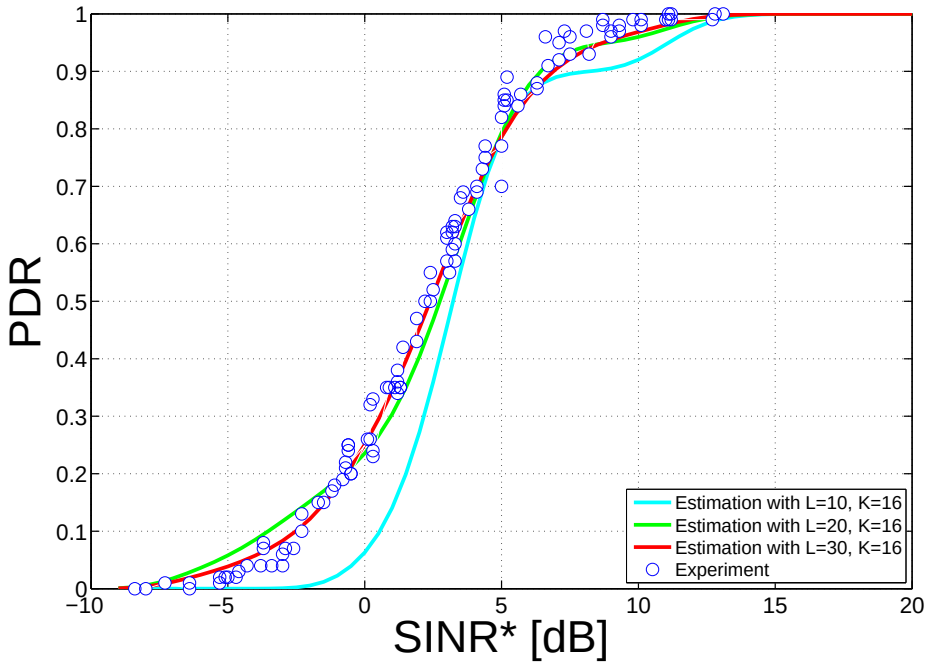

Figure 27: PDR Estimation results based on different number of macro-samples, PDR vs. SINR*, (channel model A for IEEE 802.15.4 and IEEE 802.11 links)

In the second experiment, the number of macro-samples is kept fixed, while PDR estimates are obtained by using different number of micro-samples. The receiver node collects 30 macro-samples for each estimate. Three estimates are obtained by utilizing 2, 3 and 4 micro-samples per each macro-sample. Like previous experiment, each macro-sample is collected during 1984 μs and micro-samples are uniformly collected during this time. Obviously, these numbers of micro-samples are not enough to scan the whole macro-sample windows completely and only partly covered. The PDR estimates based on different number of macro-samples and empirical PDR obtained through packet transmissions are plotted together in Figure 28.

Observation 29 (Figure 28): The estimate with four micro-samples per each macro-sample follows the empirical PDR results closely with less than 10% error, but the error is increased by using less number of macro-samples.

Observation 30 (Figure 28): The estimates with lower number of micro-samples per each macro-sample are reliable only when the SINR* is greater than 4 dB.

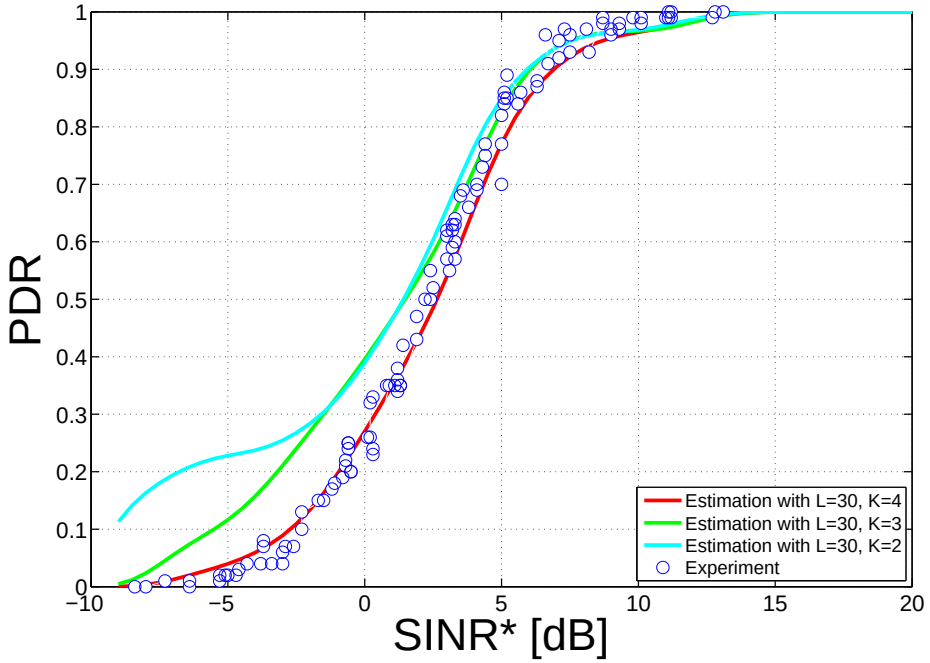

Figure 28: Estimation results based on different number of micro-samples, PDR vs. SINR*, (channel model A for IEEE 802.15.4 and IEEE 802.11 links)

These two experiments show that the number of collected samples form the channel effect directly on the accuracy of PDR estimation. It is observed that for this interferer condition, it is enough to collect about 20 macro-samples from the channel. It is also worthy to note that the entire macro-sample duration is not necessary to be scanned and collecting some samples which cover this duration partially, also provides enough accuracy. Determining the minimum number of samples from the channel is out of the scope of this thesis, but is expected that minimum number of samples depends on the channel condition, interferer activity and the desired accuracy.

5.3 Fading Channels for IEEE 802.15.4 and IEEE 802.11 Interferer

This section considers a more realistic condition which both signals from transmitter node and interferer face fading in the channel. This situation models typical wireless channels in real environments where received signal strength vary with time due to the movement of surrounding objects in the radio channel. Signals from IEEE 802.15.4 and IEEE 802.11 links experience dissimilar fading since they are normally located in different places. The only assumption we made is that channel condition varies slowly compared to the IEEE 802.15.4 packet transmission time (coherence time of the channel is greater than the IEEE 802.15.4 packet transmis-

sion time). In this condition, it can be assumed that received signal energy from IEEE 802.15.4 transmitter remains almost constant during each packet transmission, while it changes from packet to packet. The setup described in Section 3.1.3 is used to apply fading channel for both links. Channel model TGn B introduced in Section 3.4.3 is applied for the channel emulator to model fading in small environments for both links. The mobile speed is set as 3.6 km/h which is comparable with the speed of people movement in indoor environments.

In Section 4.7.2 and 4.7.3 two methods are presented to estimate the achievable PDR for such conditions: First, using the average signal strength as a common signal energy for all packets, second using the distribution of signal strength on the channel. Both of these methods need that some probe packets are transmitted in order to find received signal levels of the link in the channel. Section 5.3.1 presents the distribution of received energy from packet transmissions through the channel. Section 5.3.2 compares the PDR estimation results obtained from these two estimation methods with the empirical PDR obtained through packet transmissions.

5.3.1 Received signal strength

The received signal energy in a wireless link may vary in fading channels. Since it is required to know the received energy on the channel for PDR estimation purpose, some packet transmissions are needed to provide this information. The estimation method presented in Section 4.7.3 requires that the distribution of packet transmissions is known. To achieve this information, the IEEE 802.15.4 transmitter sends 10000 packets with inter arrival time of 30 ms. The receiver node receives packets and stores the RSSI values for successful received packets. These RSSI values are transmitted to the computer and used as the distribution of received signal strength over the channel. The distribution of RSSI values from received packets around a mean are shown in Figure 29. Since packets are transmitted in large numbers and during a long period of time, it can be expected that other packet transmissions in this fading channel have the same distribution.

5.3.2 PDR estimation results

The performance of two proposed PDR estimation algorithms for fading channels are evaluated under different interference conditions. Different traffic patterns are generated by varying the packet rates. Difference interference traffics are generated by using packet rates of 100, 300, 500 and 700 packets/sec, while payload size is kept fixed at 500 bytes. The receiver node scans the channel and collects 50 macro-samples for each traffic pattern. Macro-samples are collected every 30 ms and each one consist of 125 micro-samples. The collected samples from the channel are sent to the computer to perform PDR estimations. Two estimations are obtained based on (14) and (17). For the first estimation, average of received packets are used as the signal energy for all received packets, while for second estimation, the distribution of received packets are used as the received signal energy of packets.

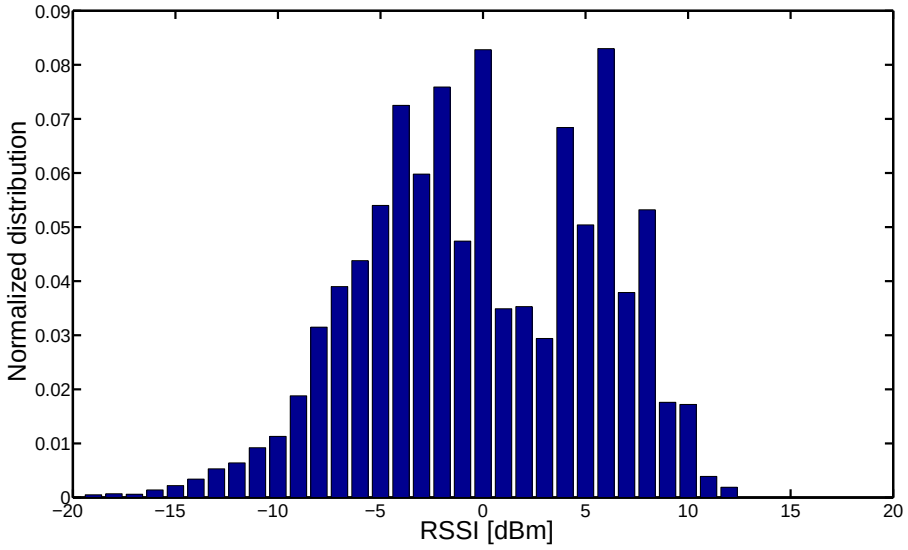

Figure 29: Normalized distribution of RSSI values from received packets, normalized density vs. RSSI

In order to compare the PDR estimation result with empirical PDR, the transmitter node sends 1000 packets, with 30 ms inter-packet time. The receiver node stores RSSI values of successful received packets and also collects RSSI sample from the channel after reception of each packet. It calculates the achieved PDR and corresponding SINR* value. The achieved PDR and the SINR* is reported to the computer to be compared with estimation results. The received signal energy from the IEEE 802.15.4 transmitter node is changed with the aid of attenuator to obtain the PDR ranging from 0 to 100%. The PDR estimations obtained from two estimator methods and empirical PDR results are plotted in Figure 30.

Observation 31 (Figure 30): The difference between PDR estimations and empirical PDR results is more, compared to previous experiments that IEEE 802.15.4 link did not fade in the channel.

Observation 32 (Figure 30): It is difficult to say for sure which one provides more accurate estimates since both estimates are close to each other. However, both of estimates follow the empirical results with less than 20% error.

Observation 33 (Figure 30): If the SINR* is greater than 10 dB, almost all the packets are successfully received by the IEEE 802.15.4 receiver regardless of the interference activity.

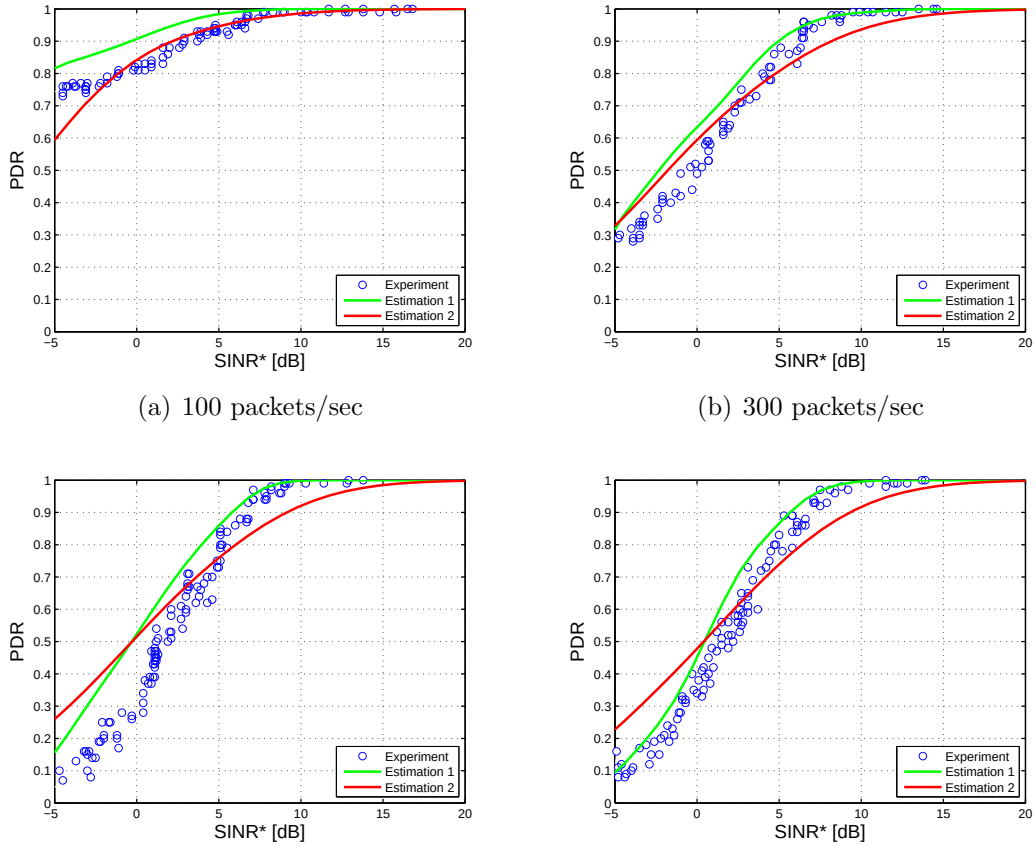

(a) 100 packets/sec

(b) 300 packets/sec

(c) 500 packets/sec

(d) 700 packets/sec

Figure 30: Estimation and empirical PDR results for variable number of packets/sec of IEEE 802.11 (with 500 bytes payload size) when both IEEE 802.15.4 and IEEE 802.11 links experience fading, PDR vs. SINR*, (channel model TGn B for IEEE 802.15.4 and IEEE 802.11 links)

5.4 Real Environment

The PDR predictions were found in good agreement with the experimental results in the emulated channels and capable of estimating the achievable PDR in the channel. It is possible to apply this algorithm in a real environment to rank all available channels. In order to verify the effectiveness of this PDR estimation algorithm on channel ranking, another experiment is carried out in an office in COMNET department. The goal of this test is to rank all 16 IEEE 802.15.4 channels in 2.4 GHz band based on PDR estimates.

5.4.1 Setup

This experiment is carried out in an office environment at the COMNET department which presents the real channel condition for a typical WSN deployment. There are two IEEE 802.11 Access Points (AP) in the office operating on IEEE 802.11 channels

1 and 6. Two laptops were placed in the office and connected to the Internet through these APs connections. They increased the traffic over specified wireless channels by downloading huge files during the experiment.

A wireless sensor link was established by using two IEEE 802.15.4 nodes located in fixed positions with a LOS connection. During the whole experiment, one of IEEE 802.15.4 nodes was used as a transmitter and the other as a receiver. The receiver node was connected to another laptop through a USB connection to log the collected data. The laptop was also equipped with a MetaGeek's Wi-Spy 2.4x module [49]. The Wi-Spy is a spectrum analyzer and captures radio activity of all wireless. The layout of the office is shown in Figure 31.

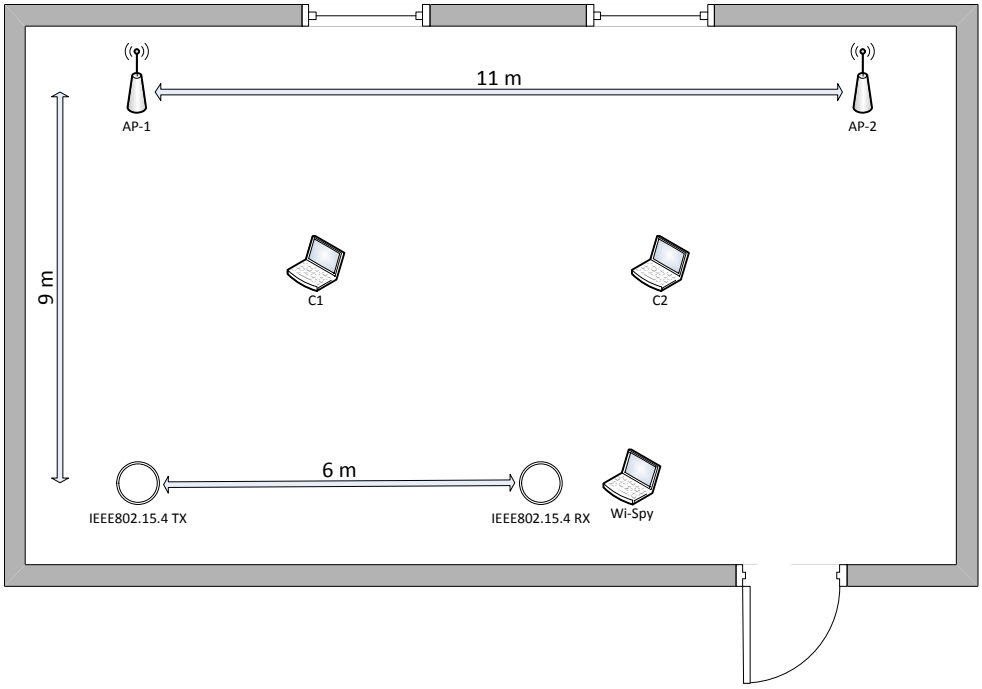

Figure 31: Layout of the office, COMNET department, Aalto University

5.4.2 Data collection

The IEEE 802.15.4 receiver node should estimate the achievable PDR for all the channels for channel ranking purpose. Hence it requires to know the received signal strength from the transmitter node and noise and interference conditions on each channel. The receiver node performs channel scanning scheme on each channel to identify noise and interference characteristics. Finally, channels are sorted based on estimated PDR values. In order to evaluate the effectiveness of channel ranking with this algorithm, channels are also ranked based on achieved empirical PDR by packet transmissions. In order to achieve these goals, following steps are repeated for each channel:

1. The IEEE 802.15.4 transmitter node sends 10 packets every second, the receiver node stores the RSSI values for received packets. These values are used as the received signal energy on the channel.

2. The IEEE 802.15.4 Receiver node scans the channel according to the channel scanning scheme presented in Section 4.5.1. It collects 20 macro-samples every 30 ms. Duration of each macro-sample is 1984 μs and consists of 16 micro-samples.

3. In order to achieve the empirical PDR on the channel, the transmitter node sends 1000 packets every 30 ms. Each packet consists of 62 bytes and transmission time of each packet is equal to 1984 μs, which is almost equal to the duration of each macro-sample. The receiver node counts the successful received packets and calculates the PDR. This step is repeated 10 times to ensure that achieved PDR is reliable.

These steps are repeated for all 16 IEEE 802.15.4 channels. Collected samples, including RSSI values from initial packet transmissions, collected macro-samples from the channels, and empirical PDR obtained through packet transmissions are transmitted to the computer.

5.4.3 Interference conditions

Before carrying out the measurement, all the channels were scanned with a Wi-Spy spectrum analyzers for 10 minutes. The spectrum utilization with wireless devices is shown Figure 32. The figure consists of three windows. The horizontal axis in all windows present the frequency labeled with IEEE 802.15.4 channels. The vertical axes in the two lowest windows present the received energy in dBm scale, while the vertical axis in the topmost window represents time. The bottommost window shows the average and the maximum perceived energy on channels during capture time. The middle window sketches the distribution of received energy on different channels while the topmost figure shows the energy level during time.

It is observed from Figure 32 that perceived energy on channels 11, 12, 13, 14, 22 and 23 are considerable and may introduce high interference for sensor link. On the other hand, it seems that there is not much significant activity on channels 25 and 26 which might promise reliable link connection for deployed sensor nodes.

5.4.4 Received signal strength

The channel responses in uncorrelated frequency channels may be different for each channel. This has a direct bearing on the average received signal strength on each channel. In order to take into account the channel response and channel fading characteristic, ten packets are transmitted by the IEEE 802.15.4 transmitter node on each channel. The receiver node stores RSSI values of the received packets. The box plot in Figure 33 illustrates distribution and the median of signal strength on each channel. The x-axis represents IEEE 802.15.4 channels while y-axis represents RSSI values obtained from CC2420 radio from the receiver node.

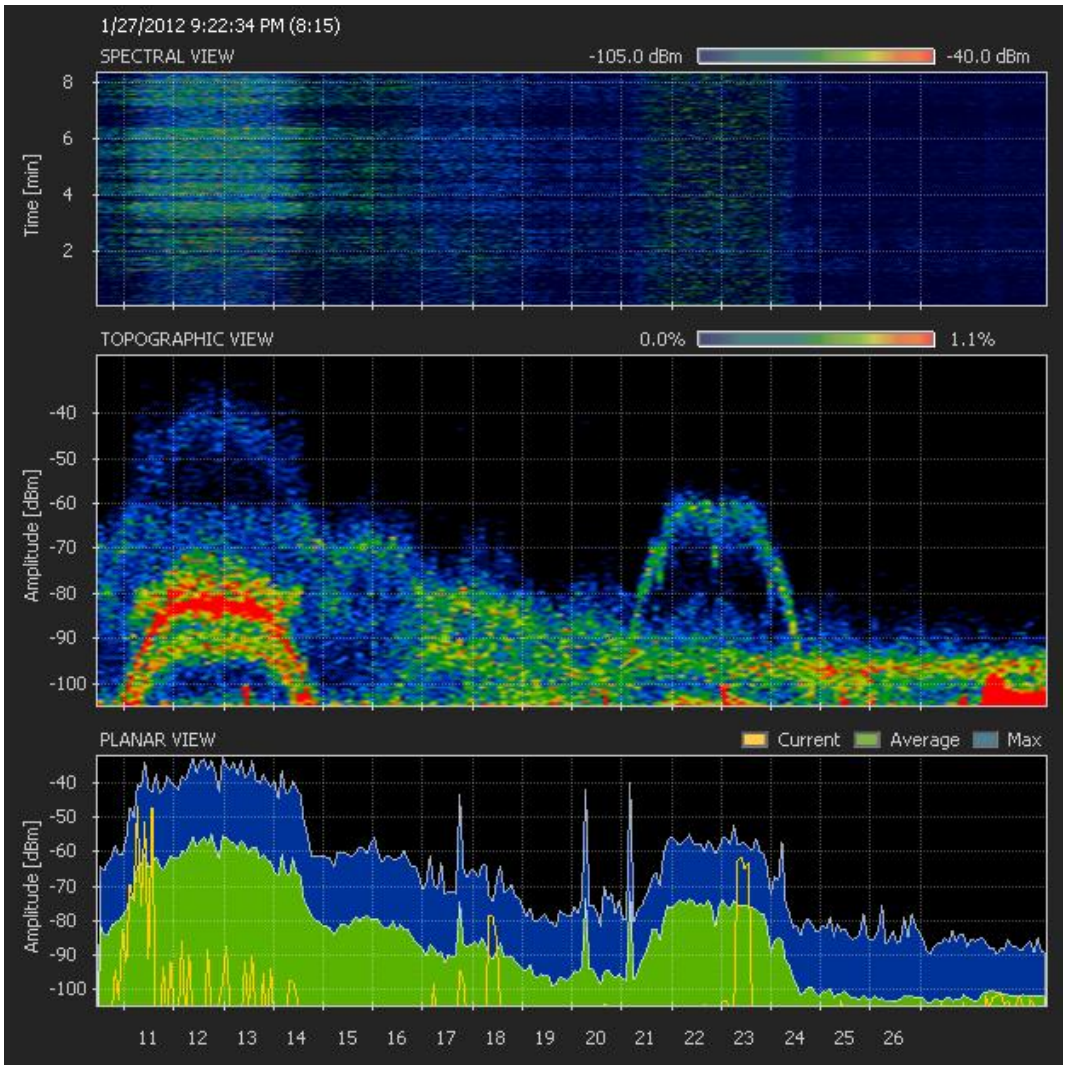

Figure 32: Interference spectrum in 2.4 GHz frequency band captured by Wi-Spy [49]

From Figure 33, it can be observed that received energy on each channel is not constant and can be changed due to fading on the channel and co-channel interference. In addition, difference between medians of RSSI values of received packets on different channels is a evidence that sensor node suffers from frequency selective fading in this indoor environment. However, channel 19 has the highest median with -85 dBm for RSSI values which indicates that this channel has the best channel response for IEEE 802.15.4 link. The lowest median is -92 dBm which belongs to channel 12, for the same reason it indicates that this channel has the worst channel response. These results confirm that channels are uncorrelated in 2.4 GHz band and received energy on each channel should be considered as well as interference conditions. The distribution of received energy on channels obtained through packet transmissions is utilized to achieve PDR estimates.

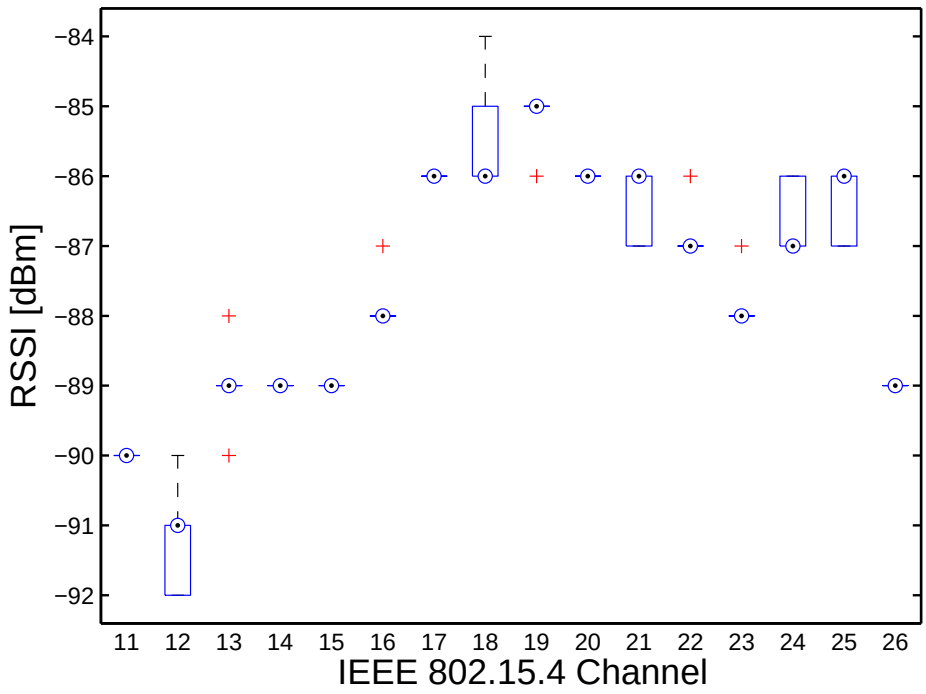

Figure 33: RSSI values of the received packets on different channels, RSSI vs. channel

5.4.5 Ranking results

After the completion of data collection, the PDR estimates have been achieved according to the methods presented in Section 4.7.2 and Section 4.7.3. The first estimates have been obtained by using the average received signal strength of received packets as signal strength for all packets and calculated based on (14) for each channel. The second estimates have been derived by using the distribution of received energy of received packets on channels and calculated based on (17). All the available channels have been sorted according to both estimates. In order to compare the estimated rank results with the actual rank of channels, channels have been also sorted based on empirical PDR achieved through packet transmissions. The PDR estimates based on two algorithms and empirical PDR achieved by transmission of 10000 packets on each channel are presented in the Table 1.

From the table, it is observed that sorting channels based on two methods have ranked them almost in the same way. This is because sensor nodes had the LOS condition and signal energy did not vary in most of the channels, consequently the average received signal energy on each channel was almost equal to the energy of individual packets. As a result, PDR estimates based on two methods remained close to each other. The difference between the estimated PDR based on two methods and empirical PDR achieved by packet transmissions on channels is less than 10%. Since

Channel Number	Actual PDR	PDR Est.1	PDR Est.2	Actual Rank	Rank Est.1	Rank Est.2
11	94	95	96	5	4	4
12	48	40	40	14	16	15
13	69	65	66	11	11	11
14	92	93	95	7	6	7
15	99	94	96	3	5	5
16	45	42	39	16	15	16
17	46	52	50	15	13	13
18	52	45	42	12	14	14
19	49	56	55	13	12	12
20	99	97	98	4	3	3
21	88	86	87	9	8	8
22	87	83	84	10	9	9
23	88	83	84	8	10	10
24	93	93	96	6	7	6
25	100	99	99	1	1	1
26	100	99	99	2	2	2

Table 1: Channel ranks of a real life environment according to PDR estimations

the achieved PDR for many channels were very close to each other, the estimated PDR could not rank all the channels in the same way that achieved PDR did. It can be observed that all the channels with more than 90% achievable PDR have been achieved high ranks between 1 and 7 through both ranking methods. Due to the low difference between estimated ranks and achieved ranks through empirical packet transmissions, the estimated ranks still can be used as a metric for channel conditions.

5.5 Application of the Channel Ranking Algorithm

The deployed channel ranking scheme has been found effective in ranking the channels for a single sensor link. However, in common WSNs, a node needs to communicate with multiple neighbor nodes. Hence it is necessary to expand the ranking scheme in order to find ranks of channels for all links of the node. Sensor nodes often transmit some packets in the network initialization to establish the network. A node can record the received energy from nodes that will intend to find channel ranks for links with them. Afterwards, it should perform channel scanning and collect samples from noise and interference on channels. These samples along with average signal energy from other nodes are enough to find rank of channels for all links. In additions, since the PDR estimator algorithm is sufficiently lightweight, and the channel ranking procedure does not make any assumption on the network topology, it can be applied to all sensor nodes to discover the optimum channel providing reliable and efficient operation of WSN.

6 Conclusion and Future Work

The proliferation of the wireless technologies, operating in 2.4 GHz ISM band, is leaving no interference-free channel for operation of low power WSNs. Channel ranking algorithm helps to find channels providing more reliable link connection. In this thesis, a PDR estimation method was proposed to rank available channels. The PDR estimation scheme is receiver oriented where a receiver node predicts the achievable PDR over a link for all candidate channels. The receiver node performs estimation based on received energy from its communication pair, noise and interference characteristics identified by channel scanning scheme.

A multipath RF-isolated test-bed was designed and implemented that enabled to emulate various wireless channel models. The proposed PDR estimation algorithm was implemented on the Sensinode sensor platforms to evaluate its accuracy under different periodic traffic patterns originated from a WLAN IEEE 802.11g interferer. Results from experiments were in a good agreements with the developed analytical framework showing desired accuracy is achievable if enough samples are collected from the channel and distribution of received signal energy from transmitter node is known. It was observed that it is possible to reduce the number of collected samples from the channel during channel scanning procedure, while the desired accuracy is met. This results in significant reduction in energy consumption of spectrum measurements. As the algorithm was found highly capable of predicting the achievable PDR on emulated channels, the algorithm was applied to rank 16 IEEE 802.15.4 channels in a real environment. It was observed that there were slightly differences between channel ranks obtained from PDR estimation method and those obtained through packet transmissions. However if the loss of PDR is considered it results in very minor degradations. In addition, since the estimator is sufficiently lightweight, it can easily be implemented in current generation wireless nodes to improve their coexistence with other collocated wireless technologies by operating on channels which proved more reliable link connection.

Future work in this area would include expansion of this algorithm to Dynamic Spectrum Access (DSA) mechanism, in which nodes switch to another high ranked channel, if the current channel does not provide the desired quality anymore. The algorithm can be utilized in multi-channel communication systems to define the highest ranked channels as the operational channel set for each link. In addition, a scanning decision approach can be developed and implemented along with the channel ranking algorithm to distinguish when the achieved ranks are not valid anymore according to current channel conditions. On this condition, node requires to perform the channel scanning procedure again in order to update ranks. The required samples from the channel during scanning procedure depends on the desired estimation accuracy, interference traffic pattern and fading in the channel. An adaptive sampling scheme can be developed to adjust the number of collected samples from the channel according to each channel condition.

References

[1] K. Romer, F. Mattern, "The design space of wireless sensor networks," IEEE Wireless Communications, Vol. 11, No. 6, pp. 54-61, December 2004.

[2] D. Yang, Y. Xu, M. Gidlund, "Wireless coexistence between IEEE 802.11- and IEEE 802.15.4-based networks: a survey," International Journal of Distributed Sensor Networks, vol. 2011.

[3] HART Communication Foundation, <http://www.hartcomm.com/>

[4] International Society for Automation, <http://www.isa.org/>

[5] A. Sikora, V.F. Groza, "Coexistence of IEEE802.15.4 with other systems in the 2.4 GHz-ISM-band," in Proceedings of the IEEE Instrumentation and Measurement Technology Conference (AMTC '05), pp. 1786-1791, May 2005.

[6] K. Srinivasan, P. Levis, "RSSI is under appreciated," in Proceedings of the Third Workshop on Embedded Networked Sensors (EmNets '06), 2006

[7] S. Han, S. Lee, S. Lee, Y. Kim, "Coexistence performance evaluation of IEEE 802.15.4 under IEEE 802.11B interference in fading channels," in Proceedings of the IEEE International Symposium on Personal, Indoor and Mobile Radio Communications (IEEE PIMRC '07), Athene, Greece, September 2007.

[8] M. Hossian, A. Mahmood, R. Jäntti, "Channel ranking algorithms for cognitive coexistence of IEEE 802.15.4," in Proceedings of the 20th IEEE International Symposium on Personal, Indoor and Mobile Radio communications, September 2009.

[9] A. Mahmood, K. Koufos , R. Jäntti, "Channel ranking algorithm and ranking error bounds: a two channel case," in Proceedings of the 22nd IEEE International Symposium on Personal Indoor and Mobile Radio communications, September 2011.

[10] C. Won, J. Youn, H. Ali, H. Sharif, J. Deogun, "Adaptive radio channel allocation for supporting coexistence of 802.15.4 and 802.11b," in Proceedings of the IEEE 62nd Vehicular Technology Conference (VTC '05), pp. 2522-2526, September 2005.

[11] S. Yoon, R. Murawski, E. Ekici, S. Park, Z.H. Mir, "Adaptive channel hopping for interference robust wireless sensor networks," in Proceedings of the IEEE International Conference on Communications (ICC), pp. 1-5, May 2010.

[12] R. Musaloiu-Elefteri, A. Terzis, "Minimising the effect of WiFi interference in 802.15.4 wireless sensor networks," International Journal of Sensor Networks, vol. 2, no. 1, pp. 43-54, 2008.

[13] D. Sexton, M. Mahony, M. Lapinski, J. Werb, "Radio channel quality in industrial wireless sensor networks," in Proceedings of the Conference on Sensors for Industry, pp. 88-94, February 2005.

[14] IEEE 802.15 WPAN Task Group 4 (TG4), <http://www.ieee802.org/15/pub/TG4.html/>

[15] IEEE standard for information technology - telecommunications and information exchange between systems - local and metropolitan area networks specific requirements part 15.4: wireless medium access control (MAC) and physical layer (PHY) specifications for low rate wireless personal area networks (LR-WPANs), IEEE Std. 802.15.4-2003.

[16] IEEE standard for information technology - telecommunications and information exchange between systems - local and metropolitan area networks specific requirements part 15.4: wireless medium access control (MAC) and physical layer (PHY) specifications for low rate wireless personal area networks (WPANs), IEEE Std. 802.15.4-2006.

[17] ZigBee Alliance, <http://www.zigbee.org/>

[18] Microchip, <http://microchip.com/stellent/>

[19] A. Castellani, N. Bui, P. Casari, M. Rossi, Z. Shelby, M. Zorzi, "Architecture and protocols for the Internet of Things: A case study," in Proceedings of the 8th IEEE International Conference on Pervasive Computing and Communications (PERCOM '10), 2010.

[20] ITU, Radiocommunication Sector, <http://itu.int/ITU-R/>

[21] J. Lorincz, D. Begusic, "Physical layer analysis of emerging IEEE 802.11n WLAN standard," in Proceedings of the 8th International Conference on Advanced Communication Technology (ICACT '06), February 2006.

[22] IEEE standard for information technology - telecommunications and information exchange between systems - local and metropolitan area networks specific requirements Part 11: Wireless LAN Medium Access Control (MAC) and Physical Layer (PHY) specifications Amendment 5: Enhancements for Higher Throughput, IEEE Std 802.11-2007.

[23] Supplement to IEEE standard for information technology - telecommunications and information exchange between systems - local and metropolitan area networks specific requirements Part 11: Wireless LAN Medium Access Control (MAC) and Physical Layer (PHY) specifications, IEEE Std 802.11n-2000.

[24] IEEE DySPAN Standards Committee (DySPAN-SC), <http://grouper.ieee.org/groups/dyspan/>

[25] M. Muck, S. Buljore, P. Martigne, A. Kousaridas, E. Patouni, M. Stamatelatos, K. Tsagkaris, J. Yang, O. Holland, "IEEE P1900.B: Coexistence Support for Reconfigurable, Heterogeneous Air Interfaces," in Proceedings of the 2nd Symposium on New Frontiers in Dynamic Spectrum Access Networks, 2007.

[26] IEEE 802.15 WPAN Task Group 2 (TG2), <http://www.ieee802.org/15/pub/TG2.html/>

[27] D. G. Yoon, S. Y. Shin, W. H. Kwon, H. S. Park, "Packet Error Rate Analysis of IEEE 802.11b under IEEE 802.15.4 Interference," in Proceedings of the IEEE 63rd Vehicular Technology Conference (VTC '06), pp. 1186-1190, July 2006.

[28] Supplement to IEEE standard for information technology - telecommunications and information exchange between systems - local and metropolitan area networks specific requirements Part 11: Wireless LAN Medium Access Control (MAC) and Physical Layer (PHY) specifications: Higher-speed physical layer extension in the 2.4 GHz Band, IEEE Std 802.11b-1999.

[29] Jennic company, "Coexistence of IEEE 802.15.4 In The 2.4GHz band application note," Tech. Rep.

[30] Sensinode, <http://www.sensinode.com/>

[31] Texas Instruments, <http://www.ti.com/product/cc2420/>

[32] Texas Instruments, <http://www.ti.com/product/msp430f1611/>

[33] Y. Chen, A. Terzis, "On the Mechanisms and Effects of Calibrating RSSI Measurements for 802.15.4 Radios," in Proceedings of the 7th European Conference on Wireless Sensor Networks (EWSN '10), pp. 256-271, February 2006.

[34] The FreeRTOS Project, <http://www.freertos.org/>

[35] Sensinode company, "NanoStack Manual," 2007.

[36] TP-LINK Technologies CO, <http://www.tp-link.com/>

[37] MadWifi, <http://madwifi-project.org/>

[38] Naval Research Laboratory, <http://pf.itd.nrl.navy.mil/mgen/mgen.html/>

[39] Qualcomm Atheros, <http://atheros.com/>

[40] Electrobit Corporation, <http://www.elektrobit.com/>

[41] J. Medbo and P. Schramm, "Channel models for HIPERLAN/2," ETSI/BRAN document no. 3ERI085B.

[42] V. Erceg, et al., "TGn Channel Models," IEEE P802.11 Wireless LANs, May 2004, doc.:IEEE 802.11-03/940r4.

[43] C. Guo, J. Zhou, P. Pawelczak, R. Hekmat, "Improving Packet Delivery Ratio Estimation for Indoor Ad Hoc and Wireless Sensor Networks," in Proceedings of the 6th IEEE Consumer Communications and Networking Conference (CCNC '09), pp. 1-5, January 2009.

[44] I. Bergel, S. Benedetto, "The effective coherence time of common channel models," in Proceedings of the IEEE Eleventh International Workshop on Signal Processing Advances in Wireless Communications (SPAWC), pp. 1-5, June 2010.

[45] A. Mahmood, R. Jäntti, "A Decision Theoretic Approach for Channel Ranking in Crowded Unlicensed Bands," International Journal of Wireless Networks, vol. 17, no. 4, pp. 907-919, May 2011.

[46] J. Hauer, A. Willig, A. Wolisz, "Mitigating the Effects of RD Interference through RSSI-Based Error Recovery," in Proceedings of the 7th European Conference on Wireless Sensor Networks (EWSN '10), pp. 224-239, June 2010.

[47] T. S. Rappaport, Prentice Hall, New York, NY, USA, 1996.

[48] M. Zuniga, B. Krishnamachari, "Analyzing the transitional region in low power wireless links," Sensor and Ad Hoc Communications and Networks, 2004, IEEE SECON 2004, Oct. 2004. in Proceedings of the First Annual IEEE Communications Society Conference on Sensor and Ad Hoc Communications and Networks (SECON '04), pp. 517-526, October 2004.

[49] MetaGeek, <http://www.metageek.net/products/wi-spy/>

Appendix A: The IEEE 802.15.4 Channels

Channel ID	Lower Frequency	Center Frequency	Upper Frequency
11	2404	2405	2406
12	2409	2410	2411
13	2414	2415	2416
14	2419	2420	2421
15	2424	2425	2426
16	2429	2430	2431
17	2434	2435	2436
18	2439	2440	2441
19	2444	2445	2446
20	2449	2450	2451
21	2454	2455	2456
22	2459	2460	2461
23	2464	2465	2466
24	2469	2470	2471
25	2474	2475	2476
26	2479	2480	2481

Table A1: The IEEE 802.15.4 channel frequencies in 2.4 GHz band

Appendix B: The IEEE 802.11 Channels

Channel ID	Lower Frequency	Center Frequency	Upper Frequency
1	2401	2412	2423
2	2404	2417	2428
3	2411	2422	2433
4	2416	2427	2438
5	2421	2432	2443
6	2426	2437	2448
7	2431	2442	2453
8	2436	2447	2458
9	2441	2452	2463
10	2446	2457	2468
11	2451	2462	2473
12	2456	2467	2478
13	2461	2472	2483
14	2473	2484	2495

Table B1: The IEEE 802.11b and IEEE 802.11g channel frequencies

Appendix C: Channel Models

Tap Number	**Delay (ns)**	**Average Power (dB)**	**Rician K**	**Doppler Spectrum**
1	0	0.0	0	Classical
2	10	-0.9	0	Classical
3	20	-1.7	0	Classical
4	30	-2.6	0	Classical
5	40	-3.5	0	Classical
6	50	-4.3	0	Classical
7	60	-5.2	0	Classical
8	70	-6.1	0	Classical
9	80	-6.9	0	Classical
10	90	-7.8	0	Classical
11	110	-4.7	0	Classical
12	140	-7.3	0	Classical
13	170	-9.9	0	Classical
14	200	-12.5	0	Classical
15	240	-13.7	0	Classical
16	290	-18.0	0	Classical
17	340	-22.4	0	Classical
18	390	-26.7	0	Classical

Table C1: Channel Model A for NLOS conditions with average 50 ns rms delay spread

Tap Number	**Delay(ns)**	**Average Power(dB)**	**Rician K**	**Doppler Spectrum**
1	0	0.0	10	Classical
2	10	-10.0	0	Classical
3	20	-10.3	0	Classical
4	30	-10.6	0	Classical
5	50	-6.4	0	Classical
6	80	-4.3	0	Classical
7	110	-8.1	0	Classical
8	140	-9.0	0	Classical
9	180	-7.9	0	Classical
10	230	-9.4	0	Classical
11	280	-10.8	0	Classical
12	330	-12.3	0	Classical
13	400	-11.7	0	Classical
14	490	-14.3	0	Classical
15	600	-15.8	0	Classical
16	730	-19.6	0	Classical
17	880	-22.7	0	Classical
18	1050	-27.6	0	Classical

Table C2: Channel Model D for LOS conditions with average 140 ns rms delay spread

Tap Number	**Delay(ns)**	**Average Power(dB)**	**Rician K**	**Doppler Spectrum**
1	0	0.0	0	Classical
2	10	-5.4	0	Classical
3	20	-2.5	0	Classical
4	30	-5.9	0	Classical
5	40	-9.2	0	Classical
6	50	-12.5	0	Classical
7	60	-15.6	0	Classical
8	70	-18.7	0	Classical
9	80	-21.8	0	Classical

Table C3: Channel Model TGn B, for smaller environments with 15 ns rms delay spread

Appendix D: C-code for High Frequency Sampling

```
int8_t rf_analyze_rssi_HF(int8_t *data,uint8_t Nsamples)
{

  uint8_t status, counter, i;
  int8_t retval = 0, temp=0;

  if (CC2420_OPEN() == pdTRUE)
  {
      CC2420_COMMAND(CC_REG_SRXON);

      status = CC2420_COMMAND_GET(CC_REG_SNOP);
      counter = 0;

      do
      {
          status = CC2420_COMMAND_GET(CC_REG_SNOP);
          status = CC2420_COMMAND_GET(CC_REG_SNOP);
      }while (!(status & CC2420_RSSI_VALID) && (counter++ < 130));

      if (!(status & CC2420_RSSI_VALID))
      {
          CC2420_STAT(status);
          retval = 0;
      }

      else
      {
          for(i=0; i<Nsamples; i++)
          {
              temp = (int8_t)CC2420_REG_GET(CC_REG_RSSI);
              temp-= 45;
              data[i]=temp;
              pause_us(16);          /* waiting one symbol period */
          }

          retval = 1;
      }

          CC2420_UNSELECT();
          CC2420_CLOSE();
  }

  return retval;
}
```

Code 1: C-code for reading RSSI samples at high frequency